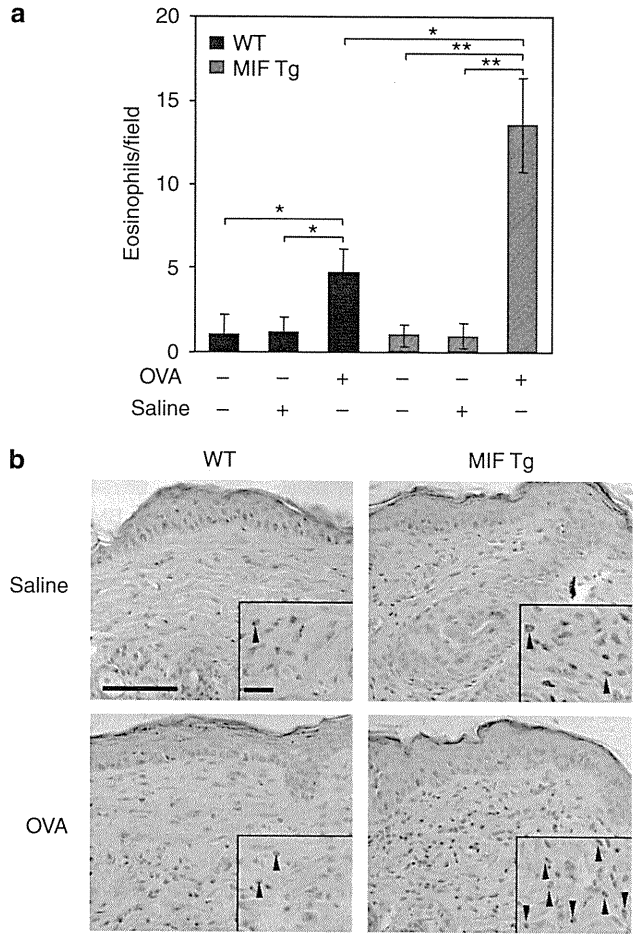

Figure 2. Eosinophil infiltration into ovalbumin (OVA)-sensitized skin sites of macrophage migration inhibitory factor (MIF) transgenic (Tg) mice. (**a**) The number of eosinophils in OVA-sensitized skin sites of MIF Tg mice was compared with the wild-type (WT) mice. Each value represents the mean ± SD ($n = 5$; $^*P < 0.001$, $^{**}P < 0.0001$). (**b**) Histological features of OVA-sensitized skin sites in MIF Tg mice and WT mice. Scale bar for large panels = 50 μm; scale bar for small panels = 10 μm; hematoxylin and eosin section. Arrowheads point to eosinophils. The experiments were repeated three times and similar results were obtained.

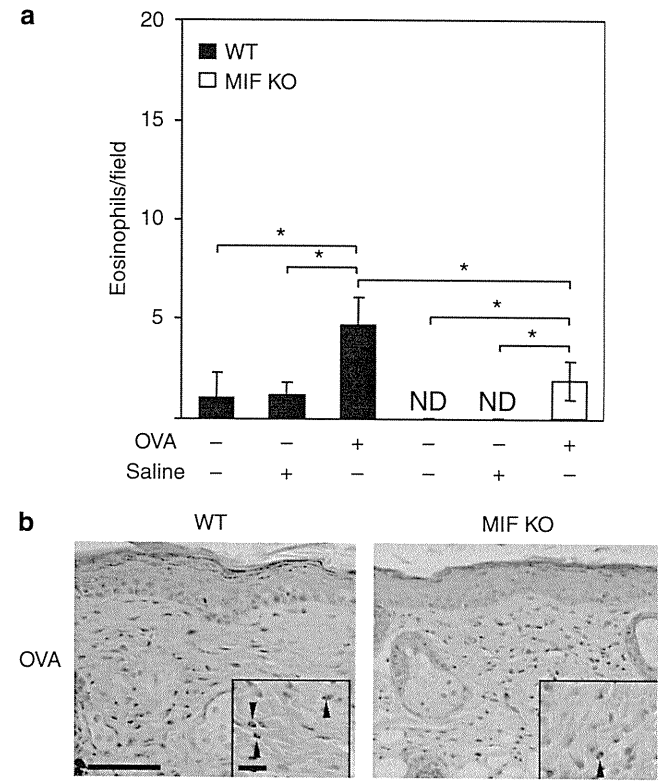

Figure 3. Eosinophil infiltration induced in ovalbumin (OVA)-sensitized skin sites of macrophage migration inhibitory factor (MIF) knockout (KO) mice. (**a**) The number of eosinophils in OVA-sensitized skin sites of MIF KO mice was compared with wild-type (WT) mice. Each value represents the mean ± SD ($n = 5$, $^*P < 0.05$). (**b**) Histological features of OVA-sensitized skin sites in MIF KO and WT mice. Scale bar for large panels = 50 μm; scale bar for small panels = 10 μm; hematoxylin and eosin section. Arrowheads point to eosinophils. The experiments were repeated three times and similar results were obtained each time.

IL-5, and IL-13, were low in the OVA-sensitized skin of MIF KO mice compared with WT mice (Figure 4).

The expression and production of eotaxin in cultured fibroblasts from MIF Tg mice and from MIF KO mice

To clarify the role of MIF in the expression of eotaxin, we performed *in vitro* experiments. A previous report described that IL-4 could dose-dependently induce the expression of eotaxin mRNA in dermal fibroblasts from humans and mice (Mochizuki *et al.*, 1998). Using this protocol, we analyzed the eotaxin expression in cultured fibroblasts from MIF Tg, MIF KO, and WT mice by stimulating them with IL-4. Unstimulated fibroblasts from these mice barely expressed eotaxin mRNA. However, fibroblasts from MIF Tg mice showed dramatically increased eotaxin mRNA after stimulation with 5 ng ml^{-1} of IL-4 (Figure 5a). To evaluate whether there was an accompanying change in eotaxin protein production, the amount of eotaxin in fibroblast supernatants was also analyzed. Eotaxin proteins in the culture supernatant of fibroblasts from MIF Tg mice were also significantly increased compared with those from WT mice ($^*P < 0.005$). However, fibroblasts from MIF KO mice showed minimal expression of eotaxin mRNA even when stimulated with 10 ng ml^{-1} of IL-4. Eotaxin production in the culture supernatant of fibroblasts from MIF KO mice was barely detectable (Figure 5b).

Recombinant MIF restored the expression and production of eotaxin in dermal fibroblasts from MIF KO mice

In dermal fibroblasts from WT mice, stimulation with IL-4 significantly induced the expression of eotaxin mRNA compared with unstimulated fibroblasts (Figure 6a). Addition of recombinant MIF significantly enhanced this increase in eotaxin expression. This suggests that the eotaxin expression in dermal fibroblasts from MIF Tg mice was markedly increased by IL-4 stimulation. A significant amount of eotaxin was also produced by combined stimulation with IL-4 ($^*P < 0.005$, $^{**}P < 0.05$; Figure 6b). Although the fibroblasts from MIF KO mice showed minimal induction of eotaxin mRNA expression in response to stimulation with IL-4, both the expression of eotaxin mRNA and the production of eotaxin protein were restored by addition of recombinant MIF

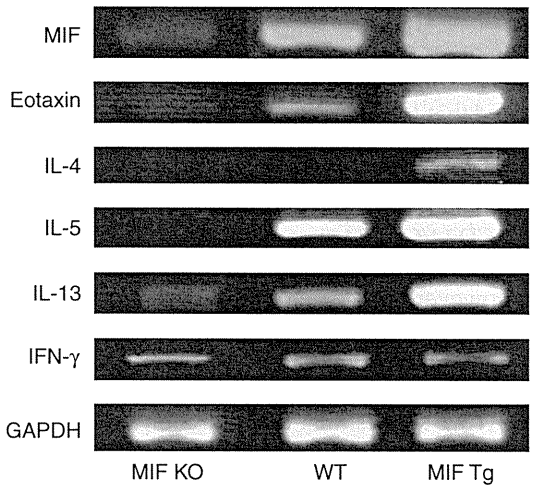

Figure 4. Expression levels of eotaxin and Th2-type cytokines in ovalbumin (OVA)-sensitized skin from macrophage migration inhibitory factor (MIF) transgenic (Tg) mice and MIF knockout (KO) mice. Reverse transcriptase-PCR analyses of eotaxin, IL-4, IL-5, IL-13, and IFN-γ levels in skin sites of MIF Tg and WT mice sensitized with OVA were performed. Eotaxin, IL-4, IL-5, and IL-13 mRNA expression levels were increased in OVA-sensitized MIF Tg; however, both eotaxin and Th2-type cytokines were markedly decreased in OVA-sensitized MIF KO mice, compared with WT mice. The experiments were repeated three times and similar results were obtained. GAPDH, glyceraldehyde-3-phosphate dehydrogenase.

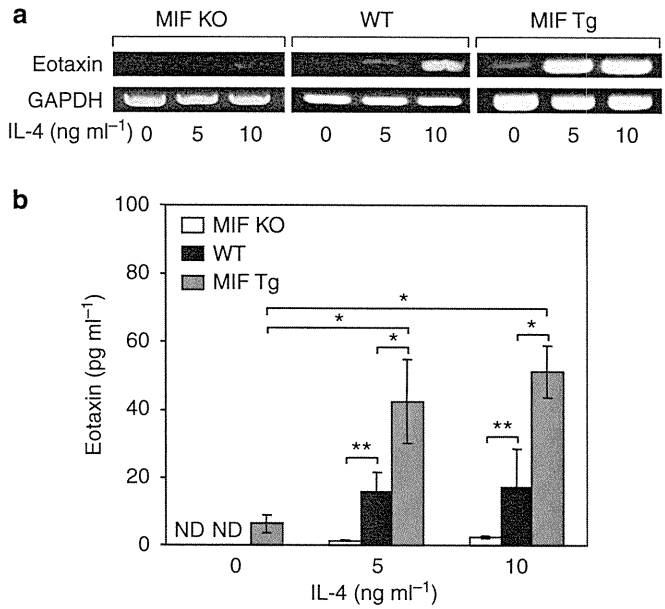

Figure 5. IL-4 induced eotaxin expression and production by fibroblasts from macrophage migration inhibitory factor (MIF) transgenic (Tg) and MIF knockout (KO) mice. Fibroblasts from MIF KO, MIF Tg, and wild-type (WT) mice were stimulated with IL-4 (5 or 10 ng ml^{-1}) for 24 hours. (**a**) RNA was extracted from the cells and the abundance of eotaxin mRNA was evaluated by reverse transcriptase-PCR. Data are from a representative experiment that was repeated three times and yielded similar results. (**b**) The eotaxin content of cultured supernatants was analyzed for eotaxin by ELISA. Each value represents the mean ± SD of five specimens. *$P<0.005$, **$P<0.05$. ND, not detected.

(Figure 6a and b). The levels of eotaxin production in MIF KO mouse fibroblasts exposed to MIF were similar to the levels in WT fibroblasts stimulated with IL-4 (Figure 6b).

DISCUSSION

There is growing evidence that the eosinophil is an important effecter cell in allergic inflammatory diseases, such as asthma and AD. Accumulation of eosinophils in the skin is characteristic of inflammation associated with AD (Leiferman, 1989; Kapp, 1995). This study explored, for the first time, the significant increase in eosinophil infiltration in the skin of MIF Tg mice after OVA sensitization, compared with WT mice. However, in MIF KO mice, eosinophils failed to infiltrate the skin after repeated epicutaneous sensitization with OVA. Eosinophils accumulate at inflammatory sites and release numerous mediators capable of initiating and maintaining allergic inflammation. Yamaguchi *et al.* (2000) reported eosinophils to be an important source of MIF in allergic inflammatory diseases. The number of eosinophils was reported to be significantly decreased in lung tissue and in bronchoalveolar lavage fluid from MIF KO mice after stimulation with OVA, compared with those from WT mice (Mizue *et al.*, 2005; Magalhães *et al.*, 2007; Wang *et al.*, 2009). In an allergic rhinitis model, eosinophil recruitment into the nasal submucosa was also suppressed in MIF KO mice (Nakamaru *et al.*, 2005). Consistent with these findings, our current evidence indicates that MIF is essential for the infiltration of eosinophils into the OVA-sensitized skin.

This study also demonstrated that the expression of both eotaxin and IL-5 is markedly increased in the OVA-sensitized

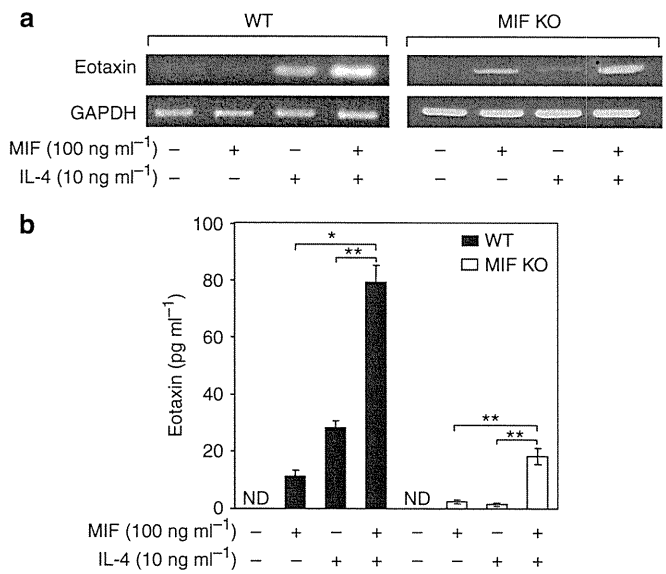

Figure 6. Recombinant macrophage migration inhibitory factor (MIF) restored eotaxin expression and production by IL-4 stimulation in dermal fibroblasts from MIF knockout (KO) mice. The fibroblasts were stimulated with IL-4 (10 ng ml^{-1}), MIF (100 ng ml^{-1}), or both IL-4 and MIF for 24 hours. (**a**) RNA was extracted from cells, and the abundance of eotaxin mRNA was evaluated by reverse transcriptase-PCR. Data are from a representative experiment that was repeated three times showing similar results. (**b**) The eotaxin contents of cultured supernatants were analyzed for eotaxin by ELISA. Each value represents the mean ± SD of six specimens. *$P<0.005$, **$P<0.05$. GAPDH, glyceraldehyde-3-phosphate dehydrogenase; ND, not detected.

skin sites of MIF Tg mice skin. The other Th2-type cytokines, IL-4 and IL-13, were also slightly increased in MIF Tg mice. On the other hand, the expression levels of eotaxin and Th2-type cytokines were markedly decreased in the OVA-sensitized skin sites of MIF KO mice. Acute AD involves a systemic Th2 response with eosinophilia, and marked infiltration of Th2 cells into skin lesions. These infiltrating T cells predominantly express IL-4, IL-5, and IL-13. Furthermore, the roles of cytokines in the induction of migration and the accumulation of eosinophils into an inflamed tissue have been extensively studied in recent years. Some of the important eosinophil chemoattractant cytokines include IL-5, IL-8, eotaxin, RANTES (regulated on activation, normal T cell expressed and secreted), and monocyte chemoattractant protein-3 (Lampinen *et al.*, 2004). Among these, eotaxin (CC chemokine ligand-11) is one of the most important eosinophil-selective chemoattractants (Jose *et al.*, 1994; Garcia-Zepeda *et al.*, 1996). Eotaxin is secreted by several cell types: epithelial cells, fibroblasts, and activated infiltrating leukocytes such as eosinophils (Garcia-Zepeda *et al.*, 1996; Ponath *et al.*, 1996; Uguccioni *et al.*, 1996). Eotaxin is reportedly related to the eosinophilia in allergic diseases, including AD and asthma (Ying *et al.*, 1997; Yawalkar *et al.*, 1999). IL-5 also has an important role in eosinophil development and differentiation (Sanderson, 1992). IL-5 KO mice had virtually no eosinophils in either saline-sensitized skin or in OVA-sensitized skin (Spergel *et al.*, 1999). Recently, Magalhães *et al.* (2009) reported that MIF was involved in IL-5-driven maturation of eosinophils and in tissue eosinophilia associated with *Schistosoma mansoni* infection. In addition, several earlier studies demonstrated that MIF KO mice failed to develop tissue eosinophilia, and that eotaxin, IL-4, and IL-5 were not induced in either allergic lung tissues or bronchoalveolar lavage fluid (Mizue *et al.*, 2005; Wang *et al.*, 2006). Accordingly, our results suggest that MIF is important in regulating both eotaxin and IL-5 in OVA-sensitized inflamed skin tissue.

In support of these *in vivo* observations, this study demonstrated that the expression of eotaxin was significantly increased after stimulation with IL-4 in fibroblasts from MIF Tg mice compared with WT fibroblasts, but not in fibroblasts from MIF KO mice. However, eotaxin expression in fibroblasts from MIF KO mice was restored by addition of recombinant MIF. These observations suggest that MIF is crucial to the expression of eotaxin, and antigen-induced eosinophil infiltration is suspected to be induced by eotaxin mainly by MIF, in addition with IL-5 production involved in MIF. Previous observations have shown that either IL-4 or IL-13 can increase eotaxin expression, and that they function synergistically with proinflammatory cytokines, such as tumor necrosis factor-α, to increase the production of eotaxin in epithelial cells and fibroblasts (Mochizuki *et al.*, 1998; Nakamura *et al.*, 1998; Li *et al.*, 1999; Stellato *et al.*, 1999; Fujisawa *et al.*, 2000; Terada *et al.*, 2000). Increases in both IL-4 and IL-13 in the inflamed skin of MIF Tg mice might involve enhancing the tissue eosinophilia. Furthermore, tumor necrosis factor-α secretion induced by MIF also has the ability to increase eotaxin expression in MIF Tg mice, on the basis of the known capacity of MIF to trigger the secretion of several inflammatory cytokines, including tumor necrosis factor-α (Donnelly *et al.*, 1997). It was recently elucidated that MIF activates an extracellular signal-regulated kinase-1/2–mitogen-activated protein kinase signaling through its receptor CD74 (Leng *et al.*, 2003) and c-Jun N-terminus kinase–mitogen-activated protein kinase signaling through CD74/CXCR4 (Lue *et al.*, 2011), in addition to the endocytic pathway described previously (Kleemann *et al.*, 2000); however, the receptor-mediated mechanism involved in MIF-mediated IL-4-induced eotaxin release is unclear. This mechanism should therefore be an important focus of research in association with MIF-mediated skin allergy.

Finally, we suggest that the inhibition of MIF might be an effective treatment for AD, suppressing both eosinophil infiltration and eotaxin expression in the skin. We recently demonstrated that in murine models of AD, MIF–DNA vaccination elicited the production of endogenous anti-MIF antibodies, producing rapid improvement of AD skin manifestations (Hamasaka *et al.*, 2009). Our previous data and the current findings therefore hold promise for the development of MIF inhibitors as a therapeutic strategy for allergic diseases.

MATERIALS AND METHODS

Materials

The following materials were obtained from commercial sources: a mouse eotaxin-specific ELISA kit from Genzyme TECHNE (Cambridge, MT); Isogen RNA extraction kit from Nippon Gene (Tokyo, Japan); M-MLV reverse transcriptase from GIBCO (Grand Island, NY); Taq DNA polymerase from Perkin-Elmer (Norwalk, CO); nylon membranes from Schleicher & Schuell (Keene, NH); Ficoll-Plaque Plus and Protein A Sepharose from Pharmacia (Uppsala, Sweden); recombinant mouse IL-4 from R&D systems (Minneapolis, MN). Recombinant rat MIF (this recombinant MIF crossreacts with that of mice) was expressed in *Escherichia coli* BL21/DE3 (Novagen, Madison, WI) and was purified as described previously (Shimizu *et al.*, 2004). All other chemicals were of analytical grade.

Mice

The MIF-overexpressing Tg mice were established after complementary DNA microinjection. Physical and biochemical characteristics, including body weight, blood pressure, and serum cholesterol and blood sugar levels, were normal, as reported previously (Sasaki *et al.*, 2004). The transgene expression was regulated by a hybrid promoter composed of the cytomegalovirus enhancer and the β-actin/β-globin promoter, as reported previously (Akagi *et al.*, 1997). The strain of the original MIF Tg mice was ICR, which were backcrossed with C57BL/6 for at least 10 generations. Tg mice were maintained by heterozygous sibling mating. Aged MIF Tg mice of 12 months or older developed neither skin allergies nor diseases. The MIF-deficient (KO) mice were established by targeted disruption of the *MIF* gene as described previously (Honma *et al.*, 2000), using a mouse strain bred onto a C57BL/6 background. MIF Tg, MIF KO, and WT mice were maintained under specific-pathogen-free conditions at the Institute for Animal Experiments of the Graduate School of Medicine and Pharmaceutical Sciences, University of Toyama. All experiments were performed on 8-week-old female adult mice.

Epicutaneous sensitization

Epicutaneous sensitization of mice was performed as described previously (Spergel *et al.*, 1998). Briefly, each mouse was anesthetized with 10% nembutal (Hospira, Osaka, Japan), then shaved with a razor. One hundred mg of OVA (Sigma, St Louis, MO) in 100 μl of normal saline were placed on a 1 × 1 cm patch (Alcare, Tokyo, Japan), which was secured to the skin with a transparent bio-occlusive dressing (ALCARE). The patch was left in place for 1 week and then removed. At the end of the second week, an identical patch was reapplied to the same skin site. Each mouse had a total of three 1-week exposures to the patch, separated from each other by 2-week intervals. Inspection confirmed that the patch was still in place at the end of each sensitization period. Skin biopsies from treated areas were obtained for RNA isolation and histological evaluation. Six-micrometer thick skin sections were stained with hematoxylin and eosin (H&E). Eosinophils were counted under a microscope at a magnification of ×400 and expressed as the mean number of the cells in five random fields (one section per mouse, five mice per group).

Northern blot analysis

Bone marrow cells were isolated from the femurs of MIF Tg or WT mice, and 1×10^6 cells ml^{-1} was collected. Total RNA was isolated from bone marrow cells and skin from mice using an Isogen RNA extraction kit according to the manufacturer's protocols. Twenty μg of RNA from control and test samples were loaded onto a formaldehyde-agarose gel and the RNA was transferred onto a nylon membrane. RNA fragments obtained by restriction enzyme treatment for MIF and glyceraldehyde-3-phosphate dehydrogenase were labeled with [α-^{32}P]deoxycytidine triphosphate using a DNA random primer labeling kit (Enzo Life Sciences International, Farmingdale, NY). Hybridization was carried out at 42 °C for 24–48 hours. Post-hybridization washing was performed in 0.1% SDS with 0.2 × standard saline citrate (1 × standard saline citrate: 0.15 M NaCl, 0.015 M sodium citrate) at 65 °C for 15 minutes. The radioactive bands were visualized by autoradiography on Kodak X-AR5 film (Tokyo, Japan) and quantitatively analyzed using the NIH Image system (Bethesda, MD). The results were normalized by compensating for the glyceraldehyde-3-phosphate dehydrogenase mRNA levels.

Reverse transcription-PCR analysis

Total RNA was extracted from each mouse skin specimen. RNA reverse transcription was performed with M-MLV reverse transcriptase using random hexamer primers and subsequent amplification using Taq DNA polymerase. PCR was carried out for 35–40 cycles with denaturation at 94 °C for 30 seconds, annealing from 46 to 64 °C for 1 minute and extension at 72 °C for 45 seconds using a thermal cycler (PE Applied Biosystems Gene Amp PCR system 9700, Life Technologies Japan, Tokyo, Japan). The primers used in this study are described in Supplementary Table S1 online. After PCR, the amplified products were analyzed by 2% agarose gel electrophoresis.

Western blot analysis

The epidermis of each mouse was homogenized with a Polytron homogenizer (Kinematica, Lausanne, Switzerland). The protein concentrations of the cell homogenates were quantified using a Micro BCA protein assay reagent kit (Thermo Fisher Scientific, Yokohama, Japan). Equal amounts of homogenates were dissolved in 20 μl of Tris-HCL, 50 mM (pH 6.8), containing 2-mercaptoethanol (1%), SDS (2%), glycerol (20%) and bromophenol blue (0.04%), and then were heated to 100 °C for 5 minutes. The samples were then subjected to SDS–PAGE and electrophoretically transferred onto a nitrocellulose membrane. The membranes were blocked with 2.5% non-fat dry milk powder in phosphate-buffered saline, probed with antibodies against MIF (Shimizu *et al.*, 1996) and subsequently reacted with secondary IgG antibodies coupled with horseradish peroxidase. The resultant complexes were processed for the ECL detection system (Amersham Biosciences, Buckinghamshire, UK). The relative amounts of proteins associated with specific antibodies were normalized according to the intensities of β-actin (Sigma).

Cell culture

Skin specimens were obtained from the dorsal surfaces of newborn MIF Tg, MIF KO, and WT mice. The skin specimens were cut into 3–5 mm pieces and placed on a large Petri dish with the subcutaneous side down, followed by tissue incubation for 1 week in a humidified atmosphere of 5% CO_2 at 37 °C. Once sufficient numbers of fibroblasts had migrated out of the skin sections, pieces of the skin were removed and the cells were passaged by trypsin digestion in the same manner as wound-harvested fibroblasts. Fibroblasts were grown in DMEM containing 10% fetal calf serum and 1% penicillin/streptomycin. After 3 passages, the fibroblasts were used for the experiments. The fibroblasts from MIF KO and WT mice were stimulated with MIF (100 ng ml^{-1}), IL-4 (10 ng ml^{-1}), or MIF (100 ng ml^{-1}) in combination with IL-4 (10 ng ml^{-1}) for 24 hours. We also stimulated the fibroblasts from MIF Tg, MIF KO, and WT mice with IL-4 (5 or 10 ng ml^{-1}) alone for 24 hours. The cells were analyzed using reverse transcriptase-PCR. Culture supernatants were analyzed for eotaxin by ELISA.

Statistical analysis

Values are expressed as the means ± SD of the respective test or control group. The statistical significance of differences between the control and test groups was evaluated by either Student's *t*-test or one-way analysis of variance.

CONFLICT OF INTEREST

The authors state no conflict of interest.

ACKNOWLEDGMENTS

This research was supported by a Grant-in-Aid for Scientific Research (Nos.11670813 and 13357008) from the Japan Society for the Promotion of Science.

SUPPLEMENTARY MATERIAL

Supplementary material is linked to the online version of the paper at http://www.nature.com/jid

REFERENCES

Akagi Y, Isaka Y, Akagi A *et al.* (1997) Transcriptional activation of a hybrid promoter composed of cytomegalovirus enhancer and beta-actin/beta-globin gene in glomerular epithelial cells *in vivo*. *Kidney Int* 51:1265–9

Bernhagen J, Calandra T, Bucala R (1998) Regulation of the immune response by macrophage migration inhibitory factor: biological and structural features. *J Mol Med* 76:151–61

Bernhagen J, Calandra T, Mitchell RA *et al.* (1993) MIF is a pituitary-derived cytokine that potentiates lethal endotoxaemia. *Nature* 365:756–9

Bloom BR, Bennett B (1966) Mechanism of reaction *in vivo* associated with delayed-type hypersensitivity. *Science* 153:80–2

Bucala R (1996) MIF re-evaluated: pituitary hormone and glucocorticoid-induced regulator of cytokine production. *FASEB J* 7:19–24

Cheng Q, McKeown SJ, Santos L *et al.* (2010) Macrophage migration inhibitory factor increases leukocyte-endothelial interactions in human endothelial cells via promotion of expression of adhesion molecules. *J Immunol* 185:1238–47

Donnelly SC, Haslett C, Reid PT *et al.* (1997) Regulatory role for macrophage migration Inhibitory factor in acute respiratory distress syndrome. *Nat Med* 3:320–3

Fujisawa T, Kato Y, Atsuta J *et al.* (2000) Chemokine production by the BEAS-2B human bronchial epithelial cells: differential regulation of eotaxin, IL-8, and RANTES by TH2- and TH1-derived cytokines. *J Allergy Clin Immunol* 105:126–33

Garcia-Zepeda EA, Rothenberg ME, Ownbey RT *et al.* (1996) Human eotaxin is a specific chemoattractant for eosinophil cells and provides a new mechanism to explain tissue eosinophilia. *Nat Med* 2:449–56

Gregory JL, Leech MT, David JR *et al.* (2004) Reduced leukocyte-endothelial cell interactions in the inflamed microcirculation of macrophage migration inhibitory factor-deficient mice. *Arthritis Rheum* 50:3023–34

Gregory JL, Morand EF, McKeown SJ *et al.* (2006) Macrophage migration inhibitory factor induces macrophage recruitment via CC chemokine ligand 2. *J Immunol* 177:8072–9

Hamasaka A, Abe R, Koyama Y *et al.* (2009) DNA vaccination against macrophage migration inhibitory factor improves atopic dermatitis in murine models. *J Allergy Clin Immunol* 124:90–9

Honma N, Koseki H, Akasaka T *et al.* (2000) Deficiency of the macrophage migration inhibitory factor gene has no significant effect on endotoxaemia. *Immunology* 100:84–90

Jose PJ, Griffiths-Johnson DA, Collins PD *et al.* (1994) Eotaxin: a potent eosinophil chemoattractant cytokine detected in a guinea pig model of allergic airways inflammation. *J Exp Med* 179:881–7

Kapp A (1995) Atopic dermatitis-the skin manifestation of atopy. *Clin Exp Allergy* 25:210–9

Kleemann R, Hausser A, Geiger R *et al.* (2000) Intracellular action of the cytokine MIF to modulate AP-1 activity and the cell cycle through Jab1. *Nature* 408:211–6

Lampinen M, Carlson M, Hakansson LD *et al.* (2004) Cytokine-regulated accumulation of eosinophils in inflammatory disease. *Allergy* 59:793–805

Leiferman KM (1989) Eosinophils in atopic dermatitis. *Allergy* 44:20–6

Leng L, Metz CN, Fang Y *et al.* (2003) MIF signal transduction initiated by binding to CD74. *J Exp Med* 197:1467–76

Leung DY, Nicklas RA, Li JT *et al.* (2004) Disease management of atopic dermatitis: an updated practice parameter. Joint Task Force on Practice Parameters. *Ann Allergy Asthma Immunol* 93:S1–21

Li L, Xia Y, Nguyen A *et al.* (1999) Effects of Th2 cytokines on chemokine expression in the lung: IL-13 potently induces eotaxin expression by airway epithelial cells. *J Immunol* 162:2477–87

Lue H, Dewor M, Leng L *et al.* (2011) Activation of the JNK signaling pathway by macrophage migration inhibitory factor (MIF) and dependence on CXCR4 and CD74. *Cell Signal* 23:135–44

Magalhães ES, Mourao-Sa DS, Vieira-de-Abreu A *et al.* (2007) Macrophage migration inhibitory factor is essential for allergic asthma but not for Th2 differentiation. *Eur J Immunol* 37:1097–106

Magalhães ES, Paiva CN, Souza HS *et al.* (2009) Macrophage migration inhibitory factor is critical to interleukin-5-driven eosinophilopoiesis and tissue eosinophilia triggered by Schistosoma mansoni infecton. *FASEB J* 23:1262–71

Mizue Y, Ghani S, Leng L *et al.* (2005) Role for macrophage migration inhibitory factor in asthma. *Proc Natl Acad Sci USA* 102:14410–5

Mochizuki M, Bartels J, Mallet AI *et al.* (1998) IL-4 induces eotaxin: a possible mechanism of selective eosinophil recruitment in helminth infection and atopy. *J Immunol* 160:60–8

Morar N, Willis-Owen SA, Moffatt MF *et al.* (2006) The genetics of atopic dermatitis. *J Allergy Clin Immunol* 118:24–34

Nakamaru Y, Oridate N, Nishihira J *et al.* (2005) Macrophage migration inhibitory factor (MIF) contributes to the development of allergic rhinitis. *Cytokine* 31:103–8

Nakamura H, Haley KJ, Nakamura T *et al.* (1998) Differential regulation of eotaxin expression by TNF-alpha and PMA in human monocytic U-937 cells. *Am J Physiol* 275:L601–10

Ponath PD, Qin S, Post TW *et al.* (1996) Molecular cloning and characterization of a human eotaxin receptor expressed selectively on eosinophils. *J Exp Med* 183:2437–48

Roger T, David J, Glauser MP *et al.* (2001) MIF regulates innate immune responses through modulation of Toll-like receptor 4. *Nature* 414:920–4

Rossi AG, Haslett C, Hirani N *et al.* (1998) Human circulating eosinophils secrete macrophage migration inhibitory factor (MIF): potential role in asthma. *J Clin Invest* 15:2869–74

Sanderson CJ (1992) Interleukin-5, eosinophils, and disease. *Blood* 79:3101–9

Sasaki S, Nishihira J, Ishibashi T *et al.* (2004) Transgene of MIF induces podocyte injury and progressive mesangial sclerosis in the mouse kidney. *Kidney Int* 65:469–81

Shimizu T (2005) Role of macrophage migration inhibitory factor (MIF) in the skin. *J Dermatol Sci* 37:65–73

Shimizu T, Abe R, Ohkawara A *et al.* (1997) Macrophage migration inhibitory factor is an essential immunoregulatory cytokine in atopic dermatitis. *Biochem Biophy Res Commun* 240:173–8

Shimizu T, Abe R, Ohkawara A *et al.* (1999) Increased production of macrophage migration inhibitory factor (MIF) by PBMCs of atopic dermatitis. *J Allergy Clin Immunol* 104:659–64

Shimizu T, Nishihira J, Watanabe H *et al.* (2004) Cetirizine, an H1-receptor antagonist, suppresses the expression of macrophage migration inhibitory factor (MIF): its potential anti-inflammatory action. *Clin Exp Allergy* 34:103–9

Shimizu T, Ohkawara A, Nishihira J *et al.* (1996) Identification of macrophage migration inhibitory factor (MIF) in human skin and its immunohistochemical localization. *FEBS Lett* 381:188–202

Spergel JM, Mizoguchi E, Brewer JP *et al.* (1998) Epicutaneous sensitization with protein antigen induces localized allergic dermatitis and hyperresponsiveness to methacholine after single exposure to aerosolized antigen in mice. *J Clin Invest* 101:1614–22

Spergel JM, Mizoguchi E, Oettgen H *et al.* (1999) Roles of TH1 and TH2 cytokines in a murine model of allergic dermatitis. *J Clin Invest* 103:1103–11

Stellato C, Matsukura S, Fal A *et al.* (1999) Differential regulation of epithelial-derived C-C chemokine expression by IL-4 and glucocorticoid budesonide. *J Immunol* 163:5624–32

Terada N, Hamano N, Nomura T *et al.* (2000) Interleukin-13 and tumor necrosis factor-a synergistically induce eotaxin production in human nasal fibroblasts. *Clin Exp Allergy* 20:348–55

Uguccioni M, Loetscher P, Forssmann U *et al.* (1996) Monocyte chemotactic protein 4 (MCP-4), a novel structural and functional analogue of MCP-3 and eotaxin. *J Exp Med* 183:2379–84

Wang B, Huang X, Wolters PJ *et al.* (2006) Cutting edge: deficiency of macrophage migration inhibitory factor impairs murine airway allergic responses. *J Immunol* 177:5779–84

Wang B, Zhang Z, Wang Y *et al.* (2009) Molecular cloning and characterization of macrophage migration inhibitory factor from small abalone Haliotis diversicolor supertexta. *Fish Shellfish Immunol* 27:57–64

Weiser WY, Temple PA, Witek-Giannotti JS *et al.* (1989) Molecular cloning of a cDNA encoding a human macrophage migration inhibitory factor. *Proc Natl Acad Sci USA* 86:7522–6

Yamaguchi E, Nishihira J, Shimizu T *et al.* (2000) Macrophage migration inhibitory factor (MIF) in bronchial asthma. *Clin Exp Allergy* 30:1244–9

Yawalkar N, Uguccioni M, Schärer J *et al.* (1999) Enhanced expression of eotaxin and CCR3 in atopic dermatitis. *J invest Dermatol* 113:43–8

Ying S, Robinson DS, Meng Q *et al.* (1997) Enhanced expression of eotaxin and CCR3 mRNA and protein in atopic athma. Association with airway hyperresponsiveness and predominant co-localization of eotaxin mRNA to bronchial epithelial and endothelial cells. *Eur J Immunol* 27:3507–16

Journal of Crohn's and Colitis (2012) 6, 215–225

Available online at www.sciencedirect.com

SciVerse ScienceDirect

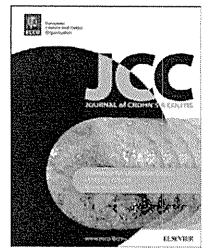

A novel NF-κB inhibitor, dehydroxymethylepoxyquinomicin, ameliorates inflammatory colonic injury in mice

Tohru Funakoshi [a], Kenichiro Yamashita [a,*,1], Nobuki Ichikawa [a], Moto Fukai [a], Tomomi Suzuki [a], Ryoichi Goto [a], Tetsu Oura [a], Nozomi Kobayashi [a], Takehiko Katsurada [b], Shin Ichihara [c], Michitaka Ozaki [d], Kazuo Umezawa [e], Satoru Todo [a,*,1]

[a] *Department of General Surgery, Graduate School of Medicine, Hokkaido University, Sapporo, Japan*
[b] *Department of Gastroenterology and Hematology, Graduate School of Medicine, Hokkaido University, Sapporo, Japan*
[c] *Department of Pathology, Sapporo-kosei General Hospital, Sapporo, Japan*
[d] *Department of Molecular Surgery, Graduate School of Medicine, Hokkaido University, Sapporo, Japan*
[e] *Department of Applied Chemistry, Keio University, Yokohama, Japan*

Received 8 March 2011; received in revised form 26 June 2011; accepted 12 August 2011

KEYWORDS
Inflammatory bowel disease;
Nuclear factor kappa B;
5-Aminosalicylic acid (5-ASA);
Experimental colitis

Abstract

Background: In inflammatory bowel disease (IBD), gut inflammation is associated with the activation of nuclear factor kappa B (NF-κB), a key pro-inflammatory transcription factor.
Aim: To investigate the therapeutic potential of a novel, specific NF-κB inhibitor, dehydroxymethylepoxyquinomicin (DHMEQ), we examined its effect on IBD using murine experimental colitis models.
Methods: The *in vitro* effect of DHMEQ was evaluated by inflammatory cytokine production and p65 immunostaining using HT-29 and RAW264.7 cells. The *in vivo* therapeutic effect of DHMEQ was studied in colitis induced by dextran sulphate sodium (DSS) and trinitrobenzenesulphonic acid (TNBS). In these, progression and severity of colitis was mainly assessed by the disease activity index (DAI), histopathology, cellular infiltration, and mRNA expression levels of pro-inflammatory cytokines in the colonic tissues.
Results: In RAW264.7 cells, DHMEQ significantly inhibited tumour necrosis factor (TNF)-α and interleukin (IL)-6 production induced by LPS in a dose-dependent manner by blocking the nuclear translocation of NF-κB. In addition, DHMEQ inhibited IL-8 production induced by LPS in HT-29 cells. DHMEQ significantly ameliorated DSS colitis as assessed by DAI scores, colonic oedema,

* Corresponding authors at: Department of General Surgery, Graduate School of Medicine, Hokkaido University N-15, W-7, Kita-ku, Sapporo 060-8638, Hokkaido, Japan. Tel.: +81 11 716 1161x5927; fax: +81 11 717 7515.
E-mail addresses: kenchan@med.hokudai.ac.jp (K. Yamashita), stodo@med.hokudai.ac.jp (S. Todo).
[1] Contributed equally as a senior author.

1873-9946/$ - see front matter
doi:10.1016/j.crohns.2011.08.011

and histological scores. Immunohistochemistry revealed that DHMEQ inhibited colonic infiltration of nuclear p65$^+$ cells, CD4$^+$ lymphocytes, and F4/80$^+$ macrophages. mRNA expression levels of the pro-inflammatory cytokines, such as IL-1β, TNF-α, IL-6, IL-12p40, IL-17, and MCP-1 were also suppressed by DHMEQ administration. Furthermore, DHMEQ significantly ameliorated TNBS colitis as assessed by body-weight changes and histological scores.
Conclusion: DHMEQ ameliorated experimental colitis in mice. These results indicate that DHMEQ appears to be an attractive therapeutic agent for IBD.

1. Introduction

Inflammatory bowel diseases (IBDs), such as Crohn's disease (CD) and ulcerative colitis (UC), are chronic, relapsing inflammatory disorders of the gastrointestinal tract that have a peak age of onset in the second to fourth decades of life. Pathogenesis of IBD involves a combination of genetic susceptibility, environmental triggers, immunological factors, and luminal microbial antigens.[1–4] Although the exact aetiologies causing IBD remain unknown, they are generally thought to result from an inappropriate and ongoing activation of the mucosal immune system against normal luminal flora. Both innate immunity responses, mainly mediated by monocytes/macrophages, and adaptive immunity responses launched by auto-reactive CD4$^+$ T cells have been postulated to play an important role in the initiation and progression of IBD.[5–7] Responding T cells exhibit a T helper type 1 (Th1) phenotype in CD and Th2 phenotype in UC.[1–4,6] Several studies have also shown that serum and mucosal interleukin (IL)-17 expressions were increased in IBD, particularly in UC.[8,9]

The transcription factor nuclear factor kappa B (NF-κB) consists of a homodimer or heterodimer of 2 subunits of the members of the NF-κB family: p65 (RelA), RelB, c-Rel, NF-κB1 (p50 and its precursor p105), or NF-κB2 (p52 and its precursor p100),[10] and plays an essential role in inflammation, cellular stress control, and cell survival/death.[11,12] Activation of cells mediating immunity, such as macrophages, dendritic cells, or lymphocytes, is chiefly regulated by NF-κB activation.[11,13,14] Furthermore, expression of anti-apoptotic molecules and of various genes which encode pro-inflammatory mediators such as cytokines, adhesion molecules, and chemokines is NF-κB dependent.[10] Dysregulation of NF-κB activity has been implicated in numerous diseases including malignancies and chronic inflammatory disorders.[12,15] In past studies, it has been shown that NF-κB is up-regulated in the inflamed human colon of CD and UC patients and plays an important role at IBD onset in experimental colitis models.[14,16] Indeed, compounds related to 5-aminosalicylic acid (5-ASA), such as sulphasalazine and mesalamine, well-known conventional therapeutic drugs for IBDs, have been shown to exert therapeutic effect in part by suppression of NF-κB activation through inhibition of phosphorylation of IκBα.[17–19] However, these drugs are not specific for suppression of NF-κB activation; furthermore, problems related to their drug delivery exist, leading to their limited efficacy for IBDs.

Dehydroxymethylepoxyquinomicin (DHMEQ) is a low-molecular-weight derivative of the antibiotic epoxyquinomycin C.[20] This novel agent has been found to inhibit DNA binding and nuclear translocation of NF-κB by covalent binding to the specific cysteine residue of the NF-κB components p65, p50, RelB, and c-Rel, but not by impairing I-κB phosphorylation or degradation.[21,22] We and others have demonstrated that administration of DHMEQ prevented cardiac allograft rejection,[23] intestinal ischaemia–reperfusion injury,[24] rheumatoid arthritis,[25] and autoimmune uveoretinitis.[26] In this study, we examined the effect of DHMEQ on IBD using murine experimental colitis models.

2. Materials and methods

2.1. Cell culture

Murine macrophage-like cell line RAW264.7 and human colon adenocarcinoma cell line HT-29 were obtained from Riken Cell Bank (Tsukuba, Japan) and the American Type Culture Collection (Rockville, MD, USA), respectively. The cells were cultured in RPMI 1640 culture media containing 2 mM L-glutamine, 100 U/mL penicillin, 100 μg/mL streptomycin, 10% foetal calf serum, and 50 μM 2-mercaptoethanol, and maintained at 37 °C in an incubator with 5% CO_2 and constant humidity.

2.2. Mice

Male C57BL/6 mice (age: 8 weeks, body weight: 22–24 g) and male BALB/c mice (age: 8 weeks, body weight: 24–26 g) were obtained from Japan SLC Inc. (Shizuoka, Japan). They were maintained under standard laboratory conditions. The experiments were approved by the Institutional Animal Care Committee, and were conducted following the guidelines of the animal care policy.

2.3. Reagents

DHMEQ was synthesised as described previously,[20,23] dissolved in dimethylsulfoxide (DMSO), and adjusted to 50 mg/mL. This stock solution was stored at −80 °C until use. For appropriate DHMEQ dose in the *in vivo* and *in vitro* experiments, the stock solution was dissolved in 0.5% carboxymethyl cellulose (CMC) solution or RPMI 1640 culture media described above. The final DMSO concentration was 4% *in vivo*, and ≤0.05% *in vitro*, respectively.

2.4. Measurement of cytokine release from cell lines

RAW264.7 (2×10^5 cells/well) and HT-29 (6×10^4 cells/well) cells in 96-well plates were incubated for 16 h. After pre-incubation, RAW264.7 cells were treated with DHMEQ for

2 h and stimulated with LPS 10 μg/mL for the desired periods of time. HT-29 cells were treated with DHMEQ for 1 h and stimulated with LPS 10 ng/mL. Supernatant was collected at 6 or 24 h after LPS stimulation and IL-6, IL-8, and tumour necrosis factor (TNF)-α levels in the supernatant were measured using an ELISA kit (R&D Systems, Minneapolis, MN, USA) following the manufacturer's instructions.

2.5. Immunocytochemistry of NF-κB in RAW264.7

RAW264.7 cells were incubated on micro slide glass for 72 h. After pre-culture, cells were treated with DHMEQ 10 μg/mL for 1 h and stimulated with LPS 10 μg/mL. Ten minutes after LPS stimulation, cells were fixed in 20% formaldehyde for 20 min. After fixing, cells were incubated with 1% H_2O_2 for 30 min, anti-p65 (Santa Cruz Biotechnology Inc., Tokyo, Japan) at 4 °C for 60 min, and treated by the EnVision plus method (K4002; Dako Ltd., Tokyo, Japan) for 30 min at room temperature, followed by visualisation with 3,3′-diaminobenzidine (DAB:K3466; Dako Ltd.) and counterstaining with haematoxylin.

2.6. Induction of colitis, treatments, and clinical assessment

2.6.1. Colitis induced by DSS

Male C57BL/6 mice (1 per cage) were given 3% dextran sulfate sodium (DSS: molecular weight = 36–50 kDa; MP Biomedicals Inc., Tokyo, Japan) in their drinking water for 5 days and thereafter provided with regular water for 5 days. Mice were intraperitoneally injected DHMEQ at a dose of 10, 20 or 40 mg/kg, or control vehicle (0.5% CMC containing with 4% DMSO) once or twice daily from day 0 to day 10. As a control therapeutic drug, 50 or 100 mg/kg of 5-ASA (Kyorin Pharmaceutical Co. Ltd., Tokyo, Japan) was intrarectally administered once per day. Body weight, stool bleeding, and stool consistency were monitored daily. Stool bleeding was assessed using Haemoccult Slide 5 Shionogi II (Shionogi & Co Ltd., Osaka, Japan). Animals were euthanised at time points and the large intestines without caecum were collected. These were weighed, measured, and evaluated for colonic oedema and microscopic damage. Severity of colitis was assessed by the disease activity index (DAI), colonic oedema (weight/length), and histological damage. The DAI was determined and scored in accordance with the method described previously.[27] Scores were calculated by grading on a scale of 0–4 the following parameters: change in weight (**0**: ≤1%, **1**: 1%–5%, **2**: 5%–10%, **3**: 10%–20%, **4**: >20%), stool bleeding (**0**: negative, **1–3**: haemoccult positive, **4**: gross bleeding), and stool consistency (**0**: normal, **1**: soft stools, **2**: loose stools, **3**: muddy stools, **4**: diarrhoea).

2.6.2. Colitis induced by TNBS

Male BALB/c mice (3 per cage) were lightly anaesthetised *via* inhalation of isoflurane, and were administered 150 μL containing 1.5 mg of trinitrobenzenesulphonic acid (TNBS; Sigma-Aldrich, Tokyo, Japan) diluted in 50% ethanol intrarectally *via* a 3.5-Fr catheter equipped with a 1-mL syringe. The catheter tip was inserted 4 cm proximal to the anal verge. To ensure proper distribution of TNBS within the entire colon and caecum, mice were kept in a vertical position for 30 s after intrarectal injection. Mice were given DHMEQ (15 mg/kg) or control vehicle (0.5% CMC containing 4% DMSO) *via* intraperitoneal injection twice daily from day 0 to day 4. The mice were euthanised on day 4 and their large intestines without caecum were collected. Progression and severity of colitis were assessed by body-weight change, colonic oedema (weight/length), macroscopic damage and histological damage of the colon. Macroscopic damage was evaluated and scored in a blinded manner as described previously,[28] according to the following criteria; **0**: normal appearance, **1**: focal hyperaemia, without ulcers, **2**: ulceration without hyperaemia or bowel wall thickening, **3**: ulceration with inflammation at one site, **4**: ulceration or inflammation at two or more sites, **5**: major sites of damage extending 1 cm along the length of the colon, **6–10**: when an area of damage extended 2 cm along the length of the colon, the score was increased by 1 for each additional cm of involvement.

2.7. Histological examination

2.7.1. Colitis induced by DSS

Specimens of whole colon without caecum were fixed in formalin and embedded in paraffin blocks. For histological examinations, 3-mm paraffin sections were stained with haematoxylin and eosin. Histological scoring of tissues was performed in a blinded manner by a skilled pathologist as described by Dieleman et al.[29] Grading index was as follows: inflammation severity (**0**: none, **1**: mild, **2**: moderate, **3**: severe), inflammation extent (**0**: none; **1**: mucosa, **2**: mucosa and submucosa, **3**: transmural), crypt damage (**0**: none, **1**: basal one-third damaged, **2**: basal two-thirds damaged, **3**: only surface epithelium intact, **4**: entire crypt and epithelium lost), and the percentage involvement in the ulcer or erosion (**1**: <1%, **2**: 1%–15%, **3**: 16%–30%, **4**: 31%–45%, **5**: 46%–100%). The sum of the first 3 scores (inflammation severity, inflammation extent, and crypt damage) was multiplied by the score of the percentage involvement.

2.7.2. Colitis induced by TNBS

Specimens of proximal colon (2.5 cm) were stained with haematoxylin and eosin. Histological scoring of tissues was performed as previously described.[30] The histological damage was categorised into 5 distinct groups, each being defined by particular levels of the following indexes; grade **0**: no signs of inflammation, grade **1**: very low level of leukocytic infiltration, grade **2**: low level of leukocytic infiltration, grade **3**: high level of leukocytic infiltration, high vascular density, and thickening of the colonic wall, grade **4**: transmural infiltrations, loss of goblet cells, high vascular density, and thickening of the colonic wall. Grading was performed in a double-blinded fashion by a skilled pathologist.

2.8. Immunohistochemistry

Three sections (distal, middle, proximal) of the colon were collected and frozen in the O.C.T. compound. For nuclear p65 staining, frozen tissue sections were cut, air dried, PFA fixed, and treated with 1% H_2O_2 for 30 min. Sections were incubated overnight at 4 °C with anti-p65 (Santa Cruz Biotechnology Inc.), and treated by the EnVision plus method (K4000; Dako Ltd.) for 30 min at room temperature, followed by visualisation

with 3,3′-diaminobenzidine (DAB:K3466; Dako Ltd.) and counterstaining with haematoxylin. To assess cellular infiltration, sections were fixed with acetone or PFA and incubated overnight at 4 °C with anti-CD4 (Santa Cruz Biotechnology Inc.), CD8 (Chemicon International Inc., Temecula, CA, USA), or F4/80 (AbD Serotec Ltd., Oxford, United Kingdom) antibodies, pre-treated with 1% H_2O_2 for 30 min. Sections were then treated with PBS, normal mouse serum, and anti-rat IgG for 30 min at room temperature and stained by the avidin–biotin complex method (PK4000; Vector Lab, Inc., Burlingame, USA), followed by visualisation with DAB (Dako Ltd.), and counterstaining with haematoxylin.

2.9. Real-time reverse-transcription polymerase chain reaction

Half of each mouse colon without caecum was snap frozen in liquid nitrogen and stored at −70 °C. Total RNA was extracted using Trizol (Invitrogen Life Technologies Japan Ltd., Tokyo, Japan) according to the manufacturer's instructions. Reverse transcription of 1 μg of total mRNA was performed at 37 °C using the Omniscript RT Kit (Qiagen K.K., Tokyo, Japan) with Oligo (dT) 20 primer (Toyobo Co Ltd., Osaka, Japan) and Protector RNase inhibitor (Roche Diagnostics K.K., Sapporo, Japan). Real-time PCR was performed on QuantiTect SYBR Green PCR Kit (Qiagen K.K.) with the LightCycler Carousel-Based System (Roche Diagnostics K.K.). PCR gene amplifications were performed using the primers listed in Table 1. Reactions were processed through 40 cycles at 94 °C for 15 s, 60 °C for 20 s, and 72 °C for 30 s. Specificity of the resulting PCR products was confirmed by melting curves after each run, and data were analysed with Roche LightCycler data analysis software from absolute plasmid DNA standards. Levels of mRNA for each sample were normalised to GAPDH and quantified relative to untreated mice.

2.10. Statistical analysis

All data were expressed as means ± SEM, except for those of $p65^+$ cell counts, TNF-α, and IL-6 concentrations that were expressed as means ± SD. Multiple group analysis of DAI and colonic oedema in DSS colitis was performed using a one-way analysis of variance with a post-hoc Tukey's test. Comparison of 2 groups in all other data was analysed by Student's *t*-test. Differences were considered statistically significant if the *P* value was less than 0.05.

3. Results

3.1. DHMEQ suppresses pro-inflammatory cytokine secretion induced by LPS by blocking the nuclear translocation of NF-κB

Initially, to define the testing dose range of DHMEQ for *in vitro* use, a direct toxicity of the agent was assessed by the 3-(4,5-dimethylthiazol-2-yl)-2,5-diphenyltetrazolium bromide (MTT) assay. DHMEQ did not exert a toxicity on the intestinal epithelial cell line, HT-29 cells when supplemented at a dose ranging from 10 to 30 μg/mL (data not shown). To confirm the inhibitory effect of DHMEQ on the nuclear translocation of NF-κB, we treated RAW264.7 cells with DHMEQ at 10 μg/mL and examined the localisation of p65 after LPS stimulation. As shown in Fig. 1A and B, DHMEQ significantly inhibited the nuclear translocation of NF-κB. In RAW264.7 cells, LPS stimulation markedly increased IL-6 and TNF-α production in the culture supernatant, whereas the levels of these cytokines were reduced by DHMEQ in a dose-dependent manner (Fig. 1C and D). Likewise, DHMEQ inhibited IL-8 production in HT-29 cells (Fig. 1E).

3.2. DHMEQ ameliorates colitis induced by DSS

To determine the therapeutic potential of DHMEQ *in vivo*, we used a murine model of colitis induced by DSS. Colitis was induced by adding 3% DSS solution for 5 days followed by regular water for 5 days with DHMEQ or control vehicle. DHMEQ treatment at a dose up to 40 mg/kg/day did not exert a considerable effect, whereas, twice daily treatment at a dose of 20 mg/kg significantly reduced the severity of

Table 1 Primers used for PCR.

Gene name	Accession number		Sequence (5′→3′)	Product size (bp)
TNF-α	NM-013693	Forward	ACCCTCACACTCAGATCATC	188
		Reverse	GAGTAGACAAGGTACAACCC	
IL-1β	NM-008361	Forward	AGCTCATATGGGTCCGACAG	174
		Reverse	GGATGAGGACATGAGCACCT	
IL-6	NM-031168	Forward	CAAAGCCAGAGTCCTTCAGAG	143
		Reverse	GCCACTCCTTCTGTGACTCC	
IL-12-p40	NM-008352	Forward	AGGAGACAGAGGAGGGGTGT	111
		Reverse	AATAGCGATCCTGAGCTTGC	
MCP-1	NM-011333	Forward	TCCCAATGAGTAGGCTGGAG	126
		Reverse	TCTGGACCCATTCCTTCTTG	
IFN-γ	NM-008337	Forward	ATCTGGAGGAACTGGCAAAA	111
		Reverse	GTTGCTGATGGCCTGATTGT	
IL-17	NM-010552	Forward	CCAGGGAGAGCTTCATCTGT	117
		Reverse	CTTGGCCTCAGTGTTTGGAC	
GAPDH	NM-008084	Forward	TACACTGAGGACCAGGTTGT	137
		Reverse	CTGTAGCCGTATTCATTGTC	

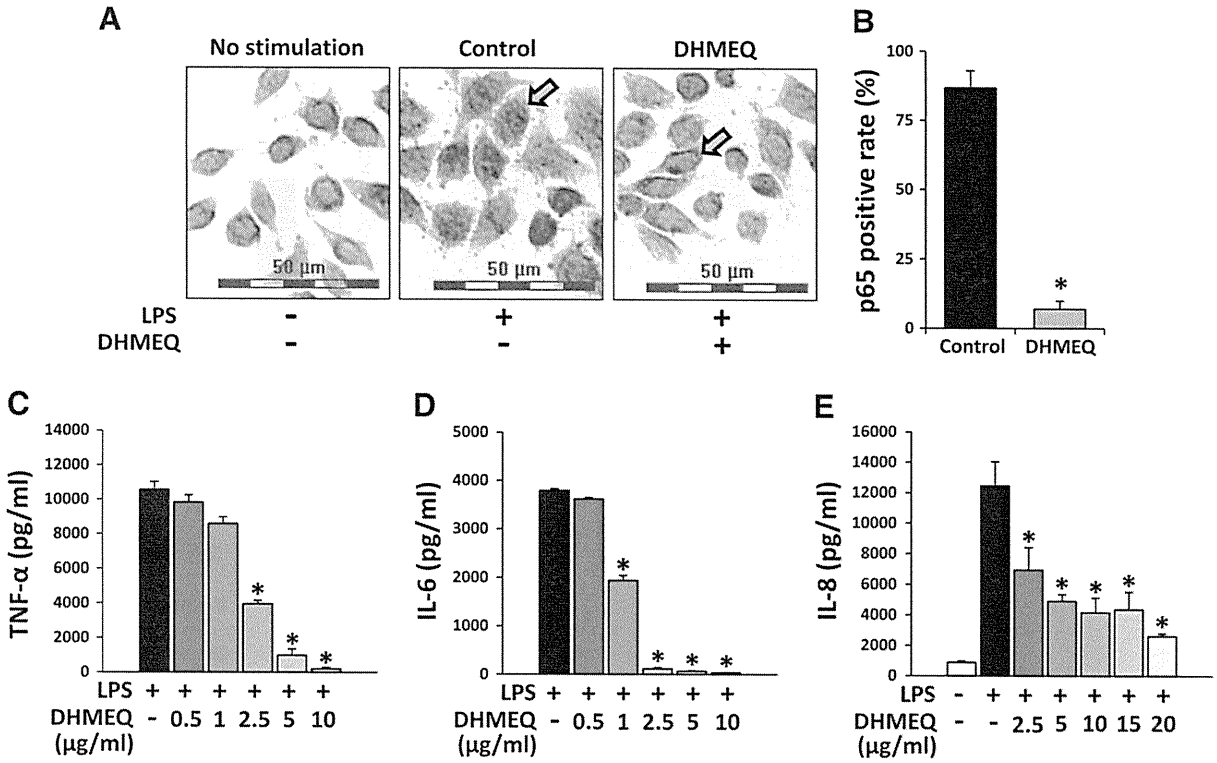

Figure 1 DHMEQ suppressed pro-inflammatory cytokine production induced by LPS by blocking the nuclear translocation of NF-κB. Localisation of NF-κB induced by LPS was studied in RAW264.7 cells. (A) Inhibition of p65 nuclear translocation in DHMEQ treatment is evident. (B) Nuclear cells positive for p65 were counted in different areas. HT-29 cells and RAW264.7 cells were incubated with the indicated concentrations of DHMEQ and LPS, respectively. Supernatants were harvested after 6 or 24 h and secreted cytokines were measured by ELISA. TNF-α (C) and IL-6 (D) production from RAW264.7, and IL-8 (E) production from HT-29 are evident. Data shown are means±SD (n=5). The asterisk indicates a statistically significant difference (*: $p<0.05$).

colitis (Fig. 2A). On day 5, control animals (given vehicle) presented a bloody, and loose stool, whilst mice treated with DHMEQ showed only occult bleeding and soft stool. The DAI score and colonic oedema, as assessed on day 10, were ameliorated by twice daily treatment with DHMEQ compared with controls (Fig. 2A and B). In contrast, 5-ASA treatment did not efficiently prevent progression of colitis induced by DSS (Fig. 2A and B).

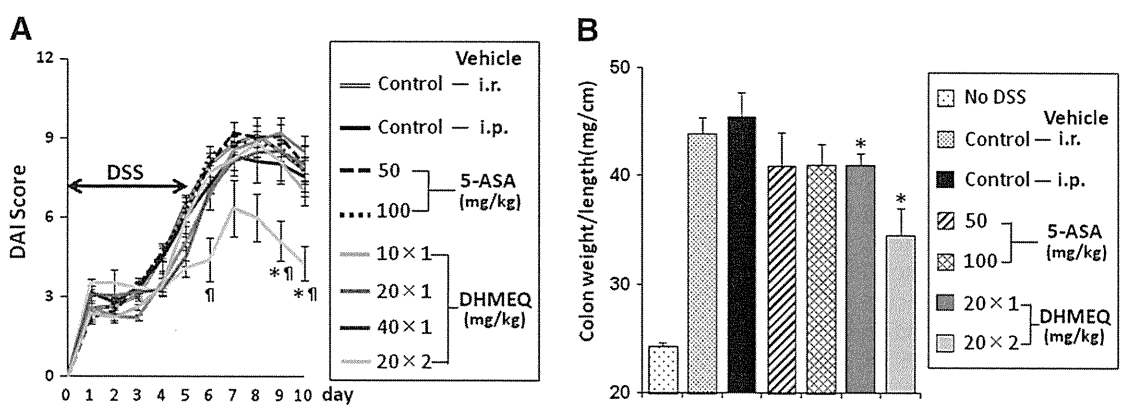

Figure 2 Effect of DHMEQ on colitis induced by DSS. C57BL/6 mice were given 3% DSS solution for 5 days, followed by regular water for 5 days. DHMEQ (10, 20 or 40 mg/kg/day) or vehicle was injected intraperitoneally once or twice daily. Comparison to 5-ASA, once daily treatment of 5-ASA (50 or 100 mg/kg) or vehicle was injected intrarectally. The effect on DAI (A) and oedema of the inflamed colon on day 10 (B) are evident. Data shown are representative of 3 independent experiments; means±SE derived from 6 mice per group. The marks indicate a statistically significant difference (*: $p<0.05$ compared to control vehicle, ¶: $p<0.05$ compared to others).

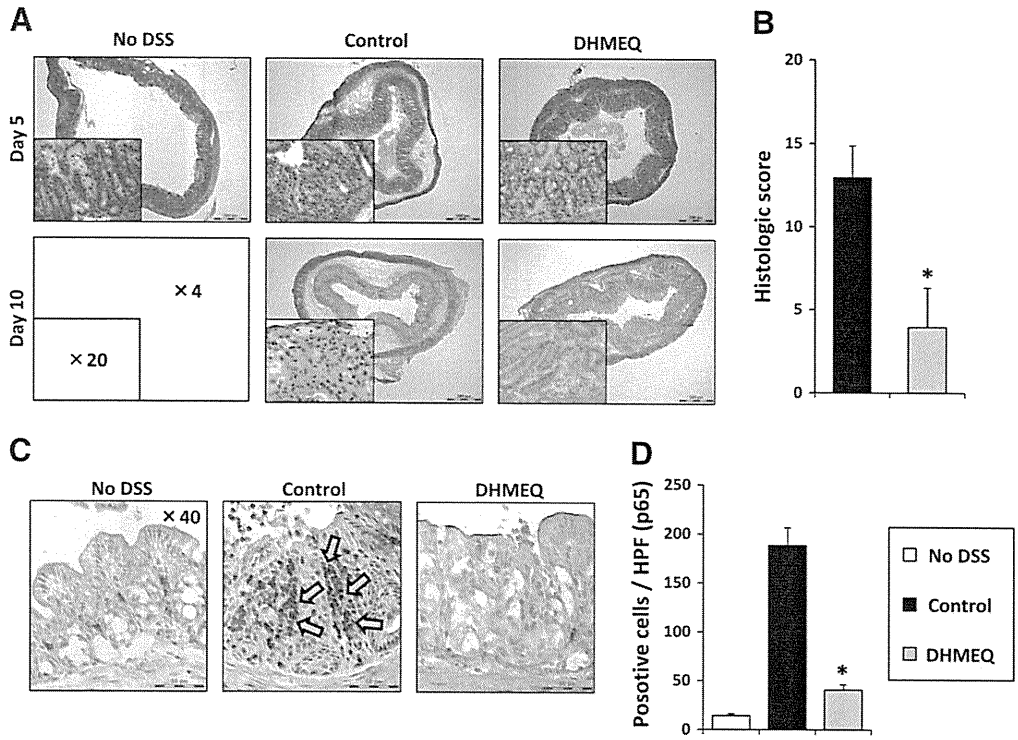

Figure 3 Effect of DHMEQ treatment on colonic tissue damage and NF-κB activity after induction of colitis induced by DSS. Mice were given 3% DSS solution for 5 days, followed by regular water for 5 days. (A) Colonic specimens on days 5 and 10 that were treated twice daily with DHMEQ (20 mg/kg) or vehicle were stained with haematoxylin and eosin. (B) The improvement in histological scores of the inflamed colon with DHMEQ treatment is evident. (C) To analyse NF-κB activity, nuclear translocation of NF-κB in colonic tissues was determined by immunostaining for p65. (D) Cells positive for nuclear p65 were counted in different areas of the colon on day 10 in mice treated with DHMEQ, controls treated with vehicle, and untreated mice. Data shown are representative of 3 independent experiments; means ± SE, 6 mice per group. The asterisk indicates a statistically significant difference (*: $p<0.05$).

3.3. DHMEQ inhibits NF-κB activity of infiltrating cells after induction of colitis mediated by DSS

The severity of colonic inflammation and ulceration was further evaluated by histopathological examination. The colons obtained from controls showed marked infiltration of inflammatory cells, loss of crypts, reduction of goblet cells, focal ulcerations, extensive destruction of mucosal layer, and submucosal oedema. In contrast, the colons of the mice treated with DHMEQ showed only mild infiltration of inflammatory cells to the mucosa, minimal loss of crypts, and reduction of goblet cells as compared to the controls (Fig. 3A). The histopathological score assessed on day 10 revealed that the degree of colitis was significantly lower in the mice treated with DHMEQ than that of controls (Fig. 3B). To further analyse NF-κB activity in inflamed colonic tissues, p65 immunostaining was performed on day 10. In the controls, nuclear p65 was positive in the inflammatory cells and epithelial cells in crypt basements. In contrast, nuclear p65 expression of inflammatory cells was significantly reduced by DHMEQ treatment, and only the cytoplasm of epithelial cells became p65 positive (Fig. 3C and D).

3.4. DHMEQ prevents colonic leukocyte infiltration

In colitis induced by DSS, it is known that macrophages and lymphocytes infiltrate into the colonic mucosa.[31,32] We thus examined cell types of infiltrating cells by immunohistochemistry. On day 5, in the control colonic tissues, infiltration into the mucosa and submucosa was mainly by $F4/80^+$ macrophages and $CD4^+$ T lymphocytes and only a few $CD8^+$ T cells (Fig. 4A). These cellular infiltrates became more intense on day 10. Compared with controls, DHMEQ significantly suppressed infiltration of these cells. The amounts of F4/80 and $CD4^+$ cells were significantly lower in mice treated with DHMEQ relative to control vehicle (Fig. 4B). In addition, there was a tendency towards much less infiltration of $CD8^+$ cells in the colons of mice treated with DHMEQ compared with controls.

3.5. DHMEQ suppresses pro-inflammatory cytokine mRNA expressions after DSS treatment

To examine whether the protection from colitis induced by DSS in mice treated with DHMEQ was associated with a decrease in the production of inflammatory molecules, RNA was extracted from colonic specimens of vehicle and mice treated with DHMEQ, and analysed for the content of various inflammatory mediators. At the end of DSS exposure on day 5, IL-1β, IL-6, TNF-α, MCP-1, IL-12p40, and IL-17 mRNA levels were significantly increased in the colons obtained from the control mice (Fig. 5). On day 10, IL-1β, IL-6, and IL-17A transcripts were further up-regulated, MCP-1 did not change, and TNF-α and IL-12p40 mRNA levels decreased. The IFN-γ transcript increased not on day 5 but on day 10. In contrast,

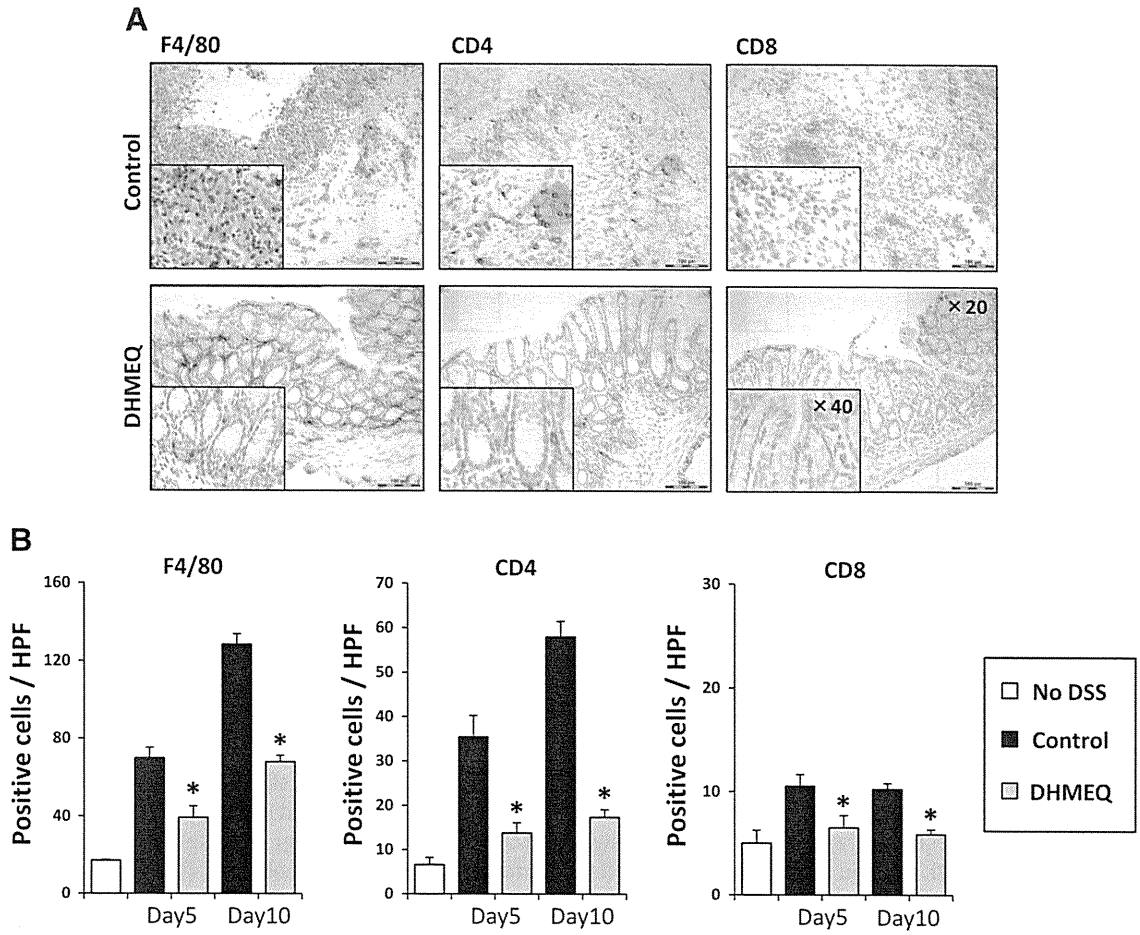

Figure 4 Protection of colitis induced by DSS in mice treated with DHMEQ is associated with a significant decrease in colonic infiltration of leukocytes. Mice were given 3% DSS solution for 5 days, followed by regular water for 5 days. DHMEQ (20 mg/kg) or vehicle was injected intraperitoneally twice daily. (A) For assessment of colonic cellular infiltration, frozen sections of colonic tissues from mice treated with DHMEQ and control mice treated with vehicle were stained with anti-CD4, anti-CD8, or anti-F4/80 antibodies. (B) Cells stained for anti-CD4, anti-CD8, or anti-F4/80 antibodies were counted in different areas of the colon on day 5 and day 10 after receiving DSS in mice treated with DHMEQ, controls, and untreated mice. Data are shown as the means±SE with 4 mice on day 5, or 6 mice on day 10 per group. The asterisk indicates a statistically significant difference (*: $p<0.05$).

DHMEQ treatment significantly reduced IL-1β, IL-6, TNF-α, IL-12p40, and IL-17A mRNA levels in the colons on day 5 as compared to those of vehicle control mice (Fig. 5). A significant suppression by DHMEQ treatment of IL-1β, IL-6, and IL-17, as well as MCP-1 and IFN-γ mRNA levels in the colon was also noted on day 10 (Fig. 5).

3.6. Treatment with DHMEQ ameliorates colitis induced by TNBS

Finally, we examined the effect of DHMEQ on colitis induced by TNBS. Treatment with DHMEQ resulted in striking protection from colitis as assessed by body-weight change, colonic oedema (weight/length), and both macroscopic and histological damages of the colon (Fig. 6). Control mice exhibited progressive body-weight loss, a characteristic sign of severe intestinal inflammation after TNBS administration, whereas mice treated with DHMEQ showed significantly less body-weight loss (Fig. 6A). DHMEQ did not ameliorate colonic oedema (Fig. 6B). Macroscopic analysis of the colon, examined on day 4, showed marked bowel wall thickening, ulceration, and inflammation in the controls. DHMEQ administration significantly improved these damages of the colon as assessed by the macroscopic score (Fig. 6C). The severity of colonic inflammation and ulceration was evaluated further by histological examinations. On day 4, transmural inflammation characterised by infiltration of inflammatory cells, predominantly neutrophils and lymphocytes, was associated with ulcerations and loss of globule cells (Fig. 6D). DHMEQ administration improved these macroscopic injuries, and restored the histological appearance of the mucosa and submucosa (Fig. 6E).

4. Discussion

In this study, we examined the anti-inflammatory property of DHMEQ in intestinal epithelial cells (IECs) and macrophages *in vitro*. Regulation of mucosal immune responses to luminal antigens is known to involve IECs.[33] They function as antigen-presenting cells to different subsets of T cells and substantially contribute to the inflammatory processes in

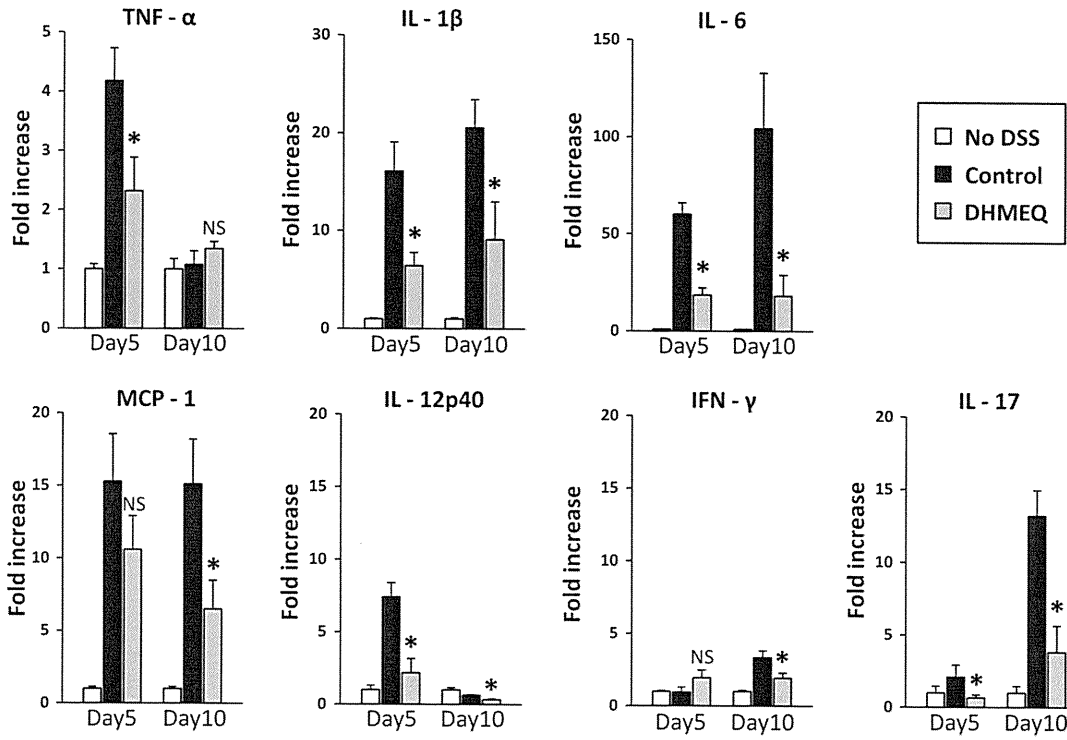

Figure 5 Protection of colitis induced by DSS in mice treated with DHMEQ is associated with a significant decrease in mRNA expression of pro-inflammatory cytokine. C57BL/6 mice were given 3% DSS solution for 5 days, followed by regular water for 5 days. DHMEQ (20 mg/kg) or vehicle was injected intraperitoneally twice daily. DHMEQ treatment (20 mg/kg), vehicle controls and no DSS mice were killed at day 5 and day 10. Colonic samples were analysed for content of the indicated molecules (TNF-α, IL-1β, IL-6, MCP-1, IL-12p40, IFN-γ, and IL-17) by real-time PCR. mRNA levels for each sample were normalised to GAPDH, then quantified relative to untreated mice. Data is shown as the means ± SE with 4 mice per group on day 5, or 6 mice per group on day 10. The asterisk indicates a statistically significant difference (*: $p<0.05$).

IBD by stimulating effector T cells and the release of IL-1, IL-6, IL-8, and TNF-α.[34,35] Of these cytokines, IL-8 is involved in the chemotaxis of neutrophils and T-cells, and it has been demonstrated that IECs overproduce IL-8 upon LPS or TNF-α stimulation *in vitro*.[36,37] In the present study, we demonstrated that DHMEQ suppressed IL-8 production induced by LPS by the HT-29 cell line.

In IBD, the intestinal lamina propria is associated with infiltration of mononuclear cells such as macrophages and lymphocytes. Macrophages, a major population of tissue-resident mononuclear phagocytes, play a key role in recognition and elimination of bacteria. Macrophages produce pro-inflammatory cytokines at the site of inflammation in response to activated Th1 cells, and induce tissue damage by enhancing mononuclear cell infiltration to the tissue.[2] In addition, dysfunction of macrophages is correlated with IBD incidence.[38] In fact, it has been reported that NOD2 mutant macrophages, which underlie the occurrence of intestinal inflammatory disease in a substantial subgroup of patients with CD, produce large amounts of IL-12 in response to stimulation with microbial components.[39,40] We have shown in the present study that DHMEQ inhibits the nuclear translocation of p65, and suppresses IL-6 and TNF-α production induced by LPS in the murine macrophage cell line RAW264.7.

To assess the *in vivo* efficacy of DHMEQ treatment on IBD, we utilised well-established models of murine colitis induced by DSS or TNBS. In the DSS colitis model, we examined the efficacy of DHMEQ at various doses. Based on our previous studies[23,24], DHMEQ was administered to animals *via* the i.p. route. Twice daily treatment with DHMEQ at 20 mg/kg/day markedly ameliorated disease activity related to colitis as assessed by DAI scores, colonic oedema, and histological damage. We also examined the efficacy of DHMEQ by intra-rectal administration in a preliminary study; however, this treatment did not show a clear effect on colitis (data not shown). In the current study, we further demonstrated the effect of DHMEQ in TNBS colitis model, which is a more aggressive model than the DSS colitis model,[41] as assessed by body-weight change, macroscopic damage, and histological damage. In addition, we compared the efficacy of DHMEQ on colitis with that of 5-ASA in order to evaluate the potential clinical utility. Previous publications reported that glucocorticoid steroids and 5-ASA are effective in preventing colitis in IBD animal models.[42,43] In comparison with 5-ASA, we found that DHMEQ was more potent than 5-ASA when examined in a DSS colitis model. This corroborates the previous finding that the NF-κB decoy, but not budesonide, ameliorated colitis in a DSS colitis model.[44] Besides the therapeutic potential of DHMEQ, no apparent side effects were noted in mice treated with DHMEQ under the current protocol. These data support our *in vitro* findings and confirm our hypothesis that inhibition of NF-κB by DHMEQ is an effective strategy for controlling colitis of IBD.

To understand the underlying mechanisms of protection mediated by DHMEQ from colitis, we investigated the colon

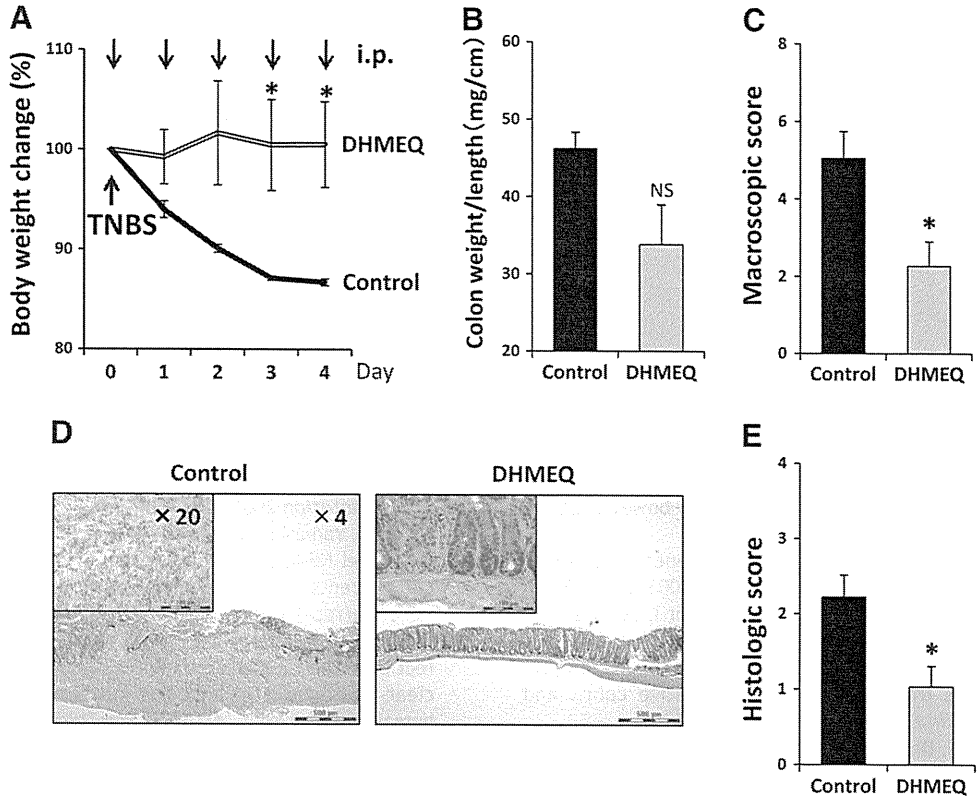

Figure 6 Treatment of colitis induced by TNBS by DHMEQ administration. Colitis was induced by rectal administration of TNBS on day 0. BALB/c mice were treated with DHMEQ or vehicle intraperitoneally twice daily. The mice were euthanised and the colons collected on day 4. (A) Body-weight curves, (B) oedema of the inflamed colons, (C) macroscopic scores of colonic tissue, (D) typical histological appearance of the colon, (F) histological scores of tissue specimens, are presented. The data shown are representative of 3 independent experiments; means ± SE for 6 mice per group. The asterisk indicates a statistically significant difference (*: $p<0.05$) compared with controls.

specimens of mice administered DSS by immunohistochemistry and real-time PCR analysis. Shortly after DSS administration, infiltration into the colon was mainly by F4/80$^+$ macrophages and CD4$^+$ T cells. This was consistent with previous reports.[31,32,45] Immunohistochemistry further revealed that many of these infiltrating cells were nuclear p65$^+$, whilst treatment with DHMEQ suppressed both cellular infiltrates and p65 expression. Corresponding to the findings by Ariga et al.[22] and our *in vitro* study, DHMEQ significantly inhibited pro-inflammatory cytokine production *in vivo* following DSS administration, as assessed by colonic mRNA expression of TNF-α, IL-1β, IL-6, and MCP-1. In conjunction with inflammation mediated by macrophages, dysregulation of T-cell response is also an important pathophysiological change in the development of IBD. In humans, cytokines associated with Th1 cells, such as IL-12 and IFN-γ, are increased in active CD patients.[6,7] Furthermore, recent study revealed that IL-17 expression in the mucosa and serum is up-regulated in active IBD patients.[8] Also, the importance of Th1/Th17 CD4$^+$ T cell response is known in chronic colitis and the delayed-phase of acute colitis induced by DSS in mice.[45–47] In the present study, DHMEQ not only suppressed infiltration of CD4$^+$ T cells in colonic mucosa, but also significantly decreased mRNA expression of molecules associated with IFN-γ, IL-12p40, and Th1/Th17 such as IL-6, IL-17, and MCP-1. These data corroborated the findings of Iwata et al., who have shown that amelioration of experimental autoimmune uveoretinitis by DHMEQ treatment was associated with inhibition of responses mediated by Th1/Th17.[26] Taken together, these data suggest that DHMEQ ameliorates colitis induced by DSS *via* suppression of macrophage and T-cell responses by blocking NF-κB activity.

Previous studies have shown that NF-κB inhibitors such as NF-κB decoy and NEMO-binding domain peptide, suppress pro-inflammatory cytokine production, and ameliorate experimental colitis.[31,44,48] In line with these reports, our present results with DHMEQ in colitis induced by both DSS and TNBS, indicate that inhibition of NF-κB activation would be a promising strategy for preventing gut inflammation. Although NF-κB decoy is anticipated for clinical applications in the area of dermatological external medicine, its molecular weight is high. In contrast, DHMEQ is a compound with low molecular weight,[20] and has shown specificity for NF-κB inhibition.[21] These characteristics of DHMEQ seem to have advantages for potential clinical applications.

In conclusion, our data provide evidence that a novel NF-κB inhibitor, DHMEQ, strongly ameliorates development of colitis. Although further studies confirming the safety and optimising treatment protocol of DHMEQ are necessary before clinical application, DHMEQ should be an attractive agent for the treatment of IBDs.

Conflict of interest statement

The authors have no conflict of interest to declare.

Acknowledgements

This study was in part supported by funding from the Promotion of Fundamental Studies in Health Sciences from the National Institute of Biomedical Innovation (NIBIO), and Grant-in-Aid for Scientific Research (C) from the Japan Society for the Promotion of Science (JSPS), Japan.

References

1. Cho JH. The genetics and immunopathogenesis of inflammatory bowel disease. *Nat Rev Immunol* 2008;**8**:458–66.
2. Sartor RB. Mechanisms of disease: pathogenesis of Crohn's disease and ulcerative colitis. *Nat Clin Pract Gastroenterol Hepatol* 2006;**3**:390–407.
3. Sartor RB. Microbial influences in inflammatory bowel diseases. *Gastroenterology* 2008;**134**:577–94.
4. Bouma G, Strober W. The immunological and genetic basis of inflammatory bowel disease. *Nat Rev Immunol* 2003;**3**:521–33.
5. Reinecker HC, Steffen M, Witthoeft T, Pflueger I, Schreiber S, MacDermott RP, et al. Enhanced secretion of tumour necrosis factor-alpha, IL-6, and IL-1 beta by isolated lamina propria mononuclear cells from patients with ulcerative colitis and Crohn's disease. *Clin Exp Immunol* 1993;**94**:174–81.
6. Fuss IJ, Neurath M, Boirivant M, Klein JS, de la Motte C, Strong SA, et al. Disparate CD4+ lamina propria (LP) lymphokine secretion profiles in inflammatory bowel disease. Crohn's disease LP cells manifest increased secretion of IFN-gamma, whereas ulcerative colitis LP cells manifest increased secretion of IL-5. *J Immunol* 1996;**157**:1261–70.
7. Monteleone G, Biancone L, Marasco R, Morrone G, Marasco O, Luzza F, et al. Interleukin 12 is expressed and actively released by Crohn's disease intestinal lamina propria mononuclear cells. *Gastroenterology* 1997;**112**:1169–78.
8. Fujino S, Andoh A, Bamba S, Ogawa A, Hata K, Araki Y, et al. Increased expression of interleukin 17 in inflammatory bowel disease. *Gut* 2003;**52**:65–70.
9. Kobayashi T, Okamoto S, Hisamatsu T, Kamada N, Chinen H, Saito R, et al. IL23 differentially regulates the Th1/Th17 balance in ulcerative colitis and Crohn's disease. *Gut* 2008;**57**:1682–9.
10. Ghosh S, Hayden MS. New regulators of NF-kappaB in inflammation. *Nat Rev Immunol* 2008;**8**:837–48.
11. Siebenlist U, Brown K, Claudio E. Control of lymphocyte development by nuclear factor-kappaB. *Nat Rev Immunol* 2005;**5**:435–45.
12. Karin M, Lin A. NF-kappaB at the crossroads of life and death. *Nat Immunol* 2002;**3**:221–7.
13. Hayden MS, West AP, Ghosh S. NF-kappaB and the immune response. *Oncogene* 2006;**25**:6758–80.
14. Rogler G, Brand K, Vogl D, Page S, Hofmeister R, Andus T, et al. Nuclear factor kappaB is activated in macrophages and epithelial cells of inflamed intestinal mucosa. *Gastroenterology* 1998;**115**:357–69.
15. Makarov SS. NF-kappaB as a therapeutic target in chronic inflammation: recent advances. *Mol Med Today* 2000;**6**:441–8.
16. Schreiber S, Nikolaus S, Hampe J. Activation of nuclear factor kappa B inflammatory bowel disease. *Gut* 1998;**42**:477–84.
17. Yan F, Polk DB. Aminosalicylic acid inhibits IkappaB kinase alpha phosphorylation of IkappaBalpha in mouse intestinal epithelial cells. *J Biol Chem* 1999;**274**:36631–6.
18. Bantel H, Berg C, Vieth M, Stolte M, Kruis W, Schulze-Osthoff K. Mesalazine inhibits activation of transcription factor NF-kappaB in inflamed mucosa of patients with ulcerative colitis. *Am J Gastroenterol* 2000;**95**:3452–7.
19. Gan HT, Chen YQ, Ouyang Q. Sulfasalazine inhibits activation of nuclear factor-kappaB in patients with ulcerative colitis. *J Gastroenterol Hepatol* 2005;**20**:1016–24.
20. Matsumoto N, Ariga A, To-e S, Nakamura H, Agata N, Hirano S, et al. Synthesis of NF-kappaB activation inhibitors derived from epoxyquinomicin C. *Bioorg Med Chem Lett* 2000;**10**:865–9.
21. Yamamoto M, Horie R, Takeiri M, Kozawa I, Umezawa K. Inactivation of NF-kappaB components by covalent binding of (−)-dehydroxymethylepoxyquinomicin to specific cysteine residues. *J Med Chem* 2008;**51**:5780–8.
22. Ariga A, Namekawa J, Matsumoto N, Inoue J, Umezawa K. Inhibition of tumor necrosis factor-alpha-induced nuclear translocation and activation of NF-kappa B by dehydroxymethylepoxyquinomicin. *J Biol Chem* 2002;**277**:24625–30.
23. Ueki S, Yamashita K, Aoyagi T, Haga S, Suzuki T, Itoh T, et al. Control of allograft rejection by applying a novel nuclear factor-kappaB inhibitor, dehydroxymethylepoxyquinomicin. *Transplantation* 2006;**82**:1720–7.
24. Suzuki T, Yamashita K, Jomen W, Ueki S, Aoyagi T, Fukai M, et al. The novel NF-kappaB inhibitor, dehydroxymethylepoxyquinomicin, prevents local and remote organ injury following intestinal ischemia/reperfusion in rats. *J Surg Res* 2008;**149**:69–75.
25. Wakamatsu K, Nanki T, Miyasaka N, Umezawa K, Kubota T. Effect of a small molecule inhibitor of nuclear factor-kappaB nuclear translocation in a murine model of arthritis and cultured human synovial cells. *Arthritis Res Ther* 2005;**7**:R1348–59.
26. Iwata D, Kitaichi N, Miyazaki A, Iwabuchi K, Yoshida K, Namba K, et al. Amelioration of experimental autoimmune uveoretinitis with nuclear factor-kappaB Inhibitor dehydroxy methyl epoxyquinomicin in mice. *Invest Ophthalmol Vis Sci* 2010;**51**:2077–84.
27. Cooper HS, Murthy SN, Shah RS, Sedergran DJ. Clinicopathologic study of dextran sulfate sodium experimental murine colitis. *Lab Invest* 1993;**69**:238–49.
28. Wallace JL, Keenan CM, Gale D, Shoupe TS. Exacerbation of experimental colitis by nonsteroidal anti-inflammatory drugs is not related to elevated leukotriene B4 synthesis. *Gastroenterology* 1992;**102**:18–27.
29. Dieleman LA, Palmen MJ, Akol H, Bloemena E, Peña AS, Meuwissen SG, et al. Chronic experimental colitis induced by dextran sulphate sodium (DSS) is characterized by Th1 and Th2 cytokines. *Clin Exp Immunol* 1998;**114**:385–91.
30. Neurath MF, Fuss I, Kelsall BL, Stüber E, Strober W. Antibodies to interleukin 12 abrogate established experimental colitis in mice. *J Exp Med* 1995;**182**:1281–90.
31. Shibata W, Maeda S, Hikiba Y, Yanai A, Ohmae T, Sakamoto K, et al. Cutting edge: the IkappaB kinase (IKK) inhibitor, NEMO-binding domain peptide, blocks inflammatory injury in murine colitis. *J Immunol* 2007;**179**:2681–5.
32. Araki A, Kanai T, Ishikura T, Makita S, Uraushihara K, Iiyama R, et al. MyD88-deficient mice develop severe intestinal inflammation in dextran sodium sulfate colitis. *J Gastroenterol* 2005;**40**:16–23.
33. Hershberg RM, Mayer LF. Antigen processing and presentation by intestinal epithelial cells — polarity and complexity. *Immunol Today* 2000;**21**:123–8.
34. Dotan I, Allez M, Nakazawa A, Brimnes J, Schulder-Katz M, Mayer L. Intestinal epithelial cells from inflammatory bowel disease patients preferentially stimulate $CD4^+$ T cells to proliferate and secrete interferon-gamma. *Am J Physiol Gastrointest Liver Physiol* 2007;**292**:G1630–40.
35. Jung HC, Eckmann L, Yang SK, Panja A, Fierer J, Morzycka-Wroblewska E, et al. A distinct array of proinflammatory cytokines is expressed in human colon epithelial cells in response to bacterial invasion. *J Clin Invest* 1995;**95**:55–65.
36. Schuerer-Maly CC, Eckmann L, Kagnoff MF, Falco MT, Maly FE. Colonic epithelial cell lines as a source of interleukin-8:

stimulation by inflammatory cytokines and bacterial lipopolysaccharide. *Immunology* 1994;**81**:85–91.
37. Sakata A, Yasuda K, Ochiai T, Shimeno H, Hikishima S, Yokomatsu T, et al. Inhibition of lipopolysaccharide-induced release of interleukin-8 from intestinal epithelial cells by SMA, a novel inhibitor of sphingomyelinase and its therapeutic effect on dextran sulphate sodium-induced colitis in mice. *Cell Immunol* 2007;**245**: 24–31.
38. Mahida YR. The key role of macrophages in the immunopathogenesis of inflammatory bowel disease. *Inflamm Bowel Dis* 2000;**6**: 21–33.
39. Hugot JP, Chamaillard M, Zouali H, Lesage S, Cézard JP, Belaiche J, et al. Association of NOD2 leucine-rich repeat variants with susceptibility to Crohn's disease. *Nature* 2001;**411**:599–603.
40. Watanabe T, Kitani A, Murray PJ, Strober W. NOD2 is a negative regulator of Toll-like receptor 2-mediated T helper type 1 responses. *Nat Immunol* 2004;**5**:800–8.
41. te Velde AA, Verstege MI, Hommes DW. Critical appraisal of the current practice in murine TNBS-induced colitis. *Inflamm Bowel Dis* 2006;**12**:995–9.
42. Nakashima T, Maeda T, Nagamoto H, Kumakura T, Takai M, Mori T. Rebamipide enema is effective for treatment of experimental dextran sulfate sodium induced colitis in rats. *Dig Dis Sci* 2005;**50**(Suppl 1):S124–31.
43. Ergang P, Leden P, Bryndová J, Zbánková S, Miksík I, Kment M, et al. Glucocorticoid availability in colonic inflammation of rat. *Dig Dis Sci* 2008;**53**:2160–7.
44. De Vry CG, Prasad S, Komuves L, Lorenzana C, Parham C, Le T, et al. Non-viral delivery of nuclear factor-kappaB decoy ameliorates murine inflammatory bowel disease and restores tissue homeostasis. *Gut* 2007;**56**:524–33.
45. Takedatsu H, Michelsen KS, Wei B, Landers CJ, Thomas LS, Dhall D, et al. TL1A (TNFSF15) regulates the development of chronic colitis by modulating both T-helper 1 and T-helper 17 activation. *Gastroenterology* 2008;**135**:552–67.
46. Melgar S, Karlsson A, Michaelsson E. Acute colitis induced by dextran sulfate sodium progresses to chronicity in C57BL/6 but not in BALB/c mice: correlation between symptoms and inflammation. *Am J Physiol Gastrointest Liver Physiol* 2005;**288**:G1328–38.
47. Fina D, Sarra M, Fantini MC, Rizzo A, Caruso R, Caprioli F, et al. Regulation of gut inflammation and th17 cell response by interleukin-21. *Gastroenterology* 2008;**134**:1038–48.
48. Fichtner-Feigl S, Fuss IJ, Preiss JC, Strober W, Kitani A. Treatment of murine Th1- and Th2-mediated inflammatory bowel disease with NF-kappa B decoy oligonucleotides. *J Clin Invest* 2005;**115**:3057–71.

World Journal of Gastroenterology

Online Submissions: http://www.wjgnet.com/1007-9327office
wjg@wjgnet.com
doi:10.3748/wjg.v18.i4.340

World J Gastroenterol 2012 January 28; 18(4): 340-348
ISSN 1007-9327 (print) ISSN 2219-2840 (online)

BRIEF ARTICLE

α-fetoprotein, vascular endothelial growth factor receptor-1 and early recurrence of hepatoma

Toshiya Kamiyama, Masato Takahashi, Kazuaki Nakanishi, Hideki Yokoo, Hirofumi Kamachi, Nozomi Kobayashi, Michitaka Ozaki, Satoru Todo

Toshiya Kamiyama, Masato Takahashi, Hideki Yokoo, Nozomi Kobayashi, Department of General Surgery, Graduate School of Medicine, Hokkaido University, North 15, West 7, Kita-ku, Sapporo 060-8638, Japan
Kazuaki Nakanishi, Hirofumi Kamachi, Satoru Todo, Department of Transplantation Surgery, Graduate School of Medicine, Hokkaido University, North 15, West 7, Kita-ku, Sapporo 060-8638, Japan
Michitaka Ozaki, Department of Molecular Surgery, Graduate School of Medicine, Hokkaido University, North 15, West 7, Kita-ku, Sapporo 060-8638, Japan
Author contributions: Kamiyama T designed the research; Kamiyama T, Takahashi M and Kobayashi N performed the research; Kamiyama T, Nakanishi K, Yokoo H, Kamachi H, Ozaki M and Todo S analyzed the data; Kamiyama T and Takahashi M wrote the paper.
Supported by Japan Society for the Promotion of Science KAKENHI 21390369 [Grant-in-Aid for Science Research (B)]
Correspondence to: Toshiya Kamiyama, MD, Department of General Surgery, Graduate School of Medicine, Hokkaido University, North 15, West 7, Kita-ku, Sapporo 060-8638, Japan. t-kamiya@med.hokudai.ac.jp
Telephone: +81-11-7065927 Fax: +81-11-7177515
Received: July 1, 2011 Revised: August 25, 2011
Accepted: August 31, 2011
Published online: January 28, 2012

Abstract

AIM: To investigate whether α-fetoprotein (AFP) and vascular endothelial growth factor receptor (VEGFR)-1 correlate with early recurrence of hepatoma/hepatocellular carcinoma (HCC).

METHODS: From 2000 to 2005, 114 consecutive patients with HCC underwent primary curative hepatectomy. The mean age was 60.7 (8.7) years and 94 patients were male. The median follow-up period was 71.2 mo (range: 43-100 mo). Immediately prior to commencing laparotomy, 5 mL bone marrow was aspirated from the sternum and collected in citrate-coated test tubes. The initial 2 mL of bone marrow aspirate was discarded in each case. AFP mRNA and VEGFR-1 mRNA in the bone marrow and peripheral blood (BM- and PH-AFP mRNA and BM- and PH-VEGFR-1 mRNA, respectively) were measured by real-time quantitative reverse transcription polymerase chain reaction. As normal controls, VEGFR-1 mRNA in the bone marrow and peripheral blood was also measured in 11 living liver donors. These data were evaluated for any correlation with early recurrence, comparing clinical and pathological outcomes.

RESULTS: The cut-off value of the BM-AFP mRNA and PH-AFP mRNA level in patients with HCC was set at 1.92 × 10^{-7} and zero, respectively, based on data from the controls. A total of 34 (29.8%) and six (5.4%) patients were positive for BM-AFP mRNA and PH-AFP mRNA, respectively. The BM-VEGFR-1 mRNA levels in all HCC patients were higher than those in the normal controls, and this was the case also for PH-VEGFR-1mRNA. The 25-percentile values for the BM- and PH-VEGFR-1 mRNA in HCC patients were used as the cut-off values for assigning the patients into two groups based on these transcript levels. The High group for BM- VEGFR-1 mRNA contained 81 (71.1%) HCC cases and the Low group was assigned 33 (28.9%) patients. These numbers for PH-VEGFR-1mRNA were 78 (75.0%) and 26 (25.0%), respectively. HCC recurred in 80 patients; in the remnant liver in 48 cases, in the remnant liver and remote tissue in 20, and in the remote tissue alone in 12. BM-AFP mRNA-positive cases showed a significantly higher rate of early recurrence (within 1 year of surgical treatment) compared with BM-AFP mRNA-negative patients (P = 0.0091). Patients were classified into four groups according to the level/status of their BM-VEGFR-1 and BM-AFP mRNA as follows: group A (n = 23), BM-VEGFR-1/BM-AFP mRNA = low/negative; group B (n = 57) high/negative; group C (n = 10) low/positive; group D (n = 24), high/positive. This classification was found to correlate with a recurrence of this

disease within 1 year (P = 0.0228). The disease-free survival curve of group A was significantly better than that of groups B, C or D (P = 0.0437, P = 0.0325, P = 0.0225). No other classification (i.e., PH-VEGF-R1/BM-AFP, BM-VEGF-R1/PH-AFP, and PH-VEGF-R1/PH-AFP mRNA) showed such a correlation.

CONCLUSION: The evaluation of BM-AFP and BM-VEGFR-1 mRNA in patients with HCC may be a valuable predictor of disease recurrence following curative resection.

Key words: α-fetoprotein; Vascular endothelial growth factor receptor-1; mRNA; Early recurrence; Hepatocellular carcinoma

Peer reviewers: Thomas Kietzmann, Professor, Dr., Department of Biochemistry, University of Oulu, FI-90014 Oulu, Finland; Arezoo Aghakhani, MD, PhD, Assistant Professor, Clinical Research Department, Pasteur Institute of Iran, No 69, Pasteur Ave., Tehran 13164, Iran

Kamiyama T, Takahashi M, Nakanishi K, Yokoo H, Kamachi H, Kobayashi N, Ozaki M, Todo S. α-fetoprotein, vascular endothelial growth factor receptor-1 and early recurrence of hepatoma. *World J Gastroenterol* 2012; 18(4): 340-348 Available from: URL: http://www.wjgnet.com/1007-9327/full/v18/i4/340.htm DOI: http://dx.doi.org/10.3748/wjg.v18.i4.340

INTRODUCTION

Various factors are thought to contribute to hepatocellular carcinoma (HCC) recurrence, which commonly results in death, including multicentric carcinogenesis in the remnant liver due to an underlying hepatitis-B-virus- or hepatitis-C-virus-induced liver cirrhosis[1], hematogenic spread, or micrometastasis of HCC cells prior to surgery or during hepatectomy by manipulation of the liver[2]. Recently, using various molecular biological markers, the detection of malignant cells in the systemic circulation and bone marrow has become possible and the presence of these cells has been found to correlate with the clinical outcome[3-8]. We have also reported from our laboratory that the detection of HCC cells in the bone marrow by real-time reverse-transcriptase polymerase chain reaction (RT-PCR) analysis of α-fetoprotein (AFP) mRNA before curative hepatectomy correlates with HCC recurrence and patient survival outcomes. Although early recurrence within 1 year of curative resection for HCC is one of the most important factors affecting the prognosis and clinical outcomes[9,10], the relationship between early recurrence and disseminated cancer cells has not yet been evaluated.

It has been recently hypothesized that metastasis is dependent on both isolated cancer cells and the host response. Kaplan *et al*[11] have reported that bone-marrow-derived hematopoietic progenitor cells that express vascular endothelial growth factor receptor (VEGFR)-1 migrate to tumor-specific pre-metastatic sites and form cellular clusters before the arrival of tumor cells both *in vitro* and *in vivo*. Moreover, it has been reported that the simultaneous presence of isolated tumor cells and VEGFR-1 expression at pre-metastatic sites is clinically significant for disease progression in gastric cancer[12]. With regard to HCC however, there has been no study to date of the association between isolated cancer cells and the expression of VEGFR-1.

In our present study, we examined whether the expression of AFP mRNA and VEGFR-1 in the bone marrow and peripheral blood, detected by sensitive real-time quantitative RT-PCR, could predict early recurrence in consecutive HCC patients who had undergone a curative hepatic resection.

MATERIALS AND METHODS

Ethics

This study was approved by the Institutional Review Board of the Hokkaido University, School of Advanced Medicine. Informed consent was obtained from each patient in accordance with the Ethics Committee Guidelines at our institution.

From July 2000 to June 2005, 114 consecutive patients underwent primary curative hepatectomy at the First Department of Surgery, Hokkaido University Hospital. The mean age was 60.7 (8.7) years and 94 patients were male. The Child-Pugh staging was A in 110 patients and B in four. Patients were discharged from the hospital at an average of 17.5 (7.1) d after surgery. They were followed up at 3-mo intervals by computed tomography (CT), magnetic resonance imaging (MRI), ultrasonography (US) and laboratory tests for AFP, lens culinaris agglutinin-reactive fraction of AFP (AFP-L3), and protein induced by vitamin K absence or antagonist-Ⅱ (PIVKA-Ⅱ). The median follow-up period was 71.2 mo (range: 43 mo-100 mo).

As normal controls, VEGFR-1 mRNA in the bone marrow and peripheral blood was also measured in 11 living liver donors. The cut-off value for AFP mRNA/glyceraldehyde-3-phosphate dehydrogenase (GAPDH) in the bone marrow and peripheral blood was set as described in our previous study[13].

Sample collections

Immediately prior to commencing the laparotomy, 5 mL bone marrow was aspirated from the sternum and collected in citrate-coated test tubes. The initial 2 mL of the bone marrow aspirate was discarded in each case.

RNA isolation and reverse transcription

Bone marrow samples were prepared for the measurement of total RNA using a Blood RNA extraction kit (QIAGEN, Hilden, Germany) according to the manufacturer's protocol with minor modifications. Briefly, 5 mL bone marrow cells were mixed with 25 mL Reagent buffer erythrocyte lysis (EL). They were then cooled on

ice for 15 min, centrifuged, and the cell pellets were collected. The pellets were suspended in 1.35 mL buffer and applied to the reagent columns, and then washed twice with reagent buffer containing ethanol. Total RNA was eluted with RNase-free water. These bone marrow RNA samples were stored at -80 ℃ until use. cDNA was generated from 1 μg total RNA using Moloney murine leukemia virus reverse transcriptase (SuperScript Ⅱ, Life Technologies, Carlsbad, CA, United States), plus 20 pmol/L each dNTP and 10 pmol/L oligo dT primers in a 20-μL final reaction volume at 42 ℃ for 1 h. This was followed by heating at 99 ℃ for 5 min.

Real-time quantitative RT-PCR

A LightCycler PCR and detection system (Roche Diagnostics, Mannheim, Germany) was used for amplification. Online quantification real-time RT-PCR was then performed in glass capillaries according to the manufacturer's protocol. The cDNA was amplified in a 20-μL PCR reaction mixture containing each dNTP (with dUTP instead of dTTP), 1 × PCR buffer, specific primers, and magnesium chloride.

For the detection of AFP, two adjacent oligonucleotide probes were used: the LightCycler Red 640 fluorophore, hAFP-LCR; (5'-CTTGCACACAAAAGCCCACTCCA-3') and a fluorophore labeled at the 3'-end with fluorescein, hAFP-FITC; (5'-TCGATCCCACTTTTCCAAGTT-3') (Nihon Gene Research Laboratories, Sendai, Japan). The sense and antisense primers (kindly supplied by Dr. Hiroaki Nagano at Osaka University) used for the amplification of AFP were as follows: 5'-TGCAGCCAAAGTGAAGAGGGAAGA-3') (hAFP-s) and 5'-CATAGCGAGCAGCCCAAAGAAGAA-3' (hAFP-As). The RT-PCR amplification was carried out for one cycle of 95 ℃ for 10 min, followed by 35 cycles of 95 ℃ for 10 s, 62 ℃ for 15 s, and 72 ℃ for 15 s. The final cycle was followed by a 10-min extension step at 40 ℃.

For the detection of VEGFR-1, two adjacent oligonucleotide probes were used: hVEGFR-1-LCR; 5'-TTCCGTGTCCCCACTGCCAA-3' and hVEGFR-1-FITC; 5'-GGGAAGCTCACTGGCATGGC-3'. The sense and antisense primers for the amplification of VEGFR-1 were as follows: 5'-TCATGAATGTTTCCCTGCAA-3' (h VEGFR-1-S) and 5'-GGAGGTATGGTGCTTCCTGA-3' (h VEGFR-1-As). These primers were designed using sequences described in a previous report[14]. RT-PCR amplification was carried out for one cycle of 95 ℃ for 10 min, followed by 35 cycles of 95 ℃ for 10 s, 60 ℃ for 10 s, and 72 ℃ for 16 s. The final cycle was followed by a 10-min extension step at 40 ℃.

For the detection of GAPDH as an internal control, two adjacent oligonucleotide probes were used: hGAPDH-LCR; 5'-TTCCGTGTCCCCACTGCCAA-3' and hGAPDH-FITC; 5'-GGGAAGCTCACTGGCATGGC-3'. The sense and antisense primers for the amplification of GAPDH were as follows: 5'-GCCTCCTGCACCACCAACTG-3' (hGAPDH-S) and 5'-CGACGCCTGCTTCACCACCTTCT-3' (hGAPDH-As). The RT-PCR amplification was carried out for one cycle of 95 ℃ for 10 min, followed by 35 cycles of 95 ℃ for 10 s, 60 ℃ for 10 s and 72 ℃ for 16 s. The final cycle was followed by a 10-min extension step at 40 ℃.

Quantification analysis

Quantification data were analyzed using the LightCycler analysis software (Roche Diagnostics, Mannheim, Germany) in accordance with the manufacturer's instructions. In this analysis, the background fluorescence was removed by setting a noise band. The crossing point for the calculation of amplified PCR products was set by the intersection of the best-fit line through the log-linear lesion and the noise band. The standard curve was a plot of the "crossing point" versus the copy number of DNA fragments inserted into the cloning vector.

Statistical analysis

Cumulative survival and disease-free survival (DFS) rates were computed according to the Kaplan-Meier method and compared between groups using the Breslow-Gehan-Wilcoxon test. The Cox proportional hazards model was used for multivariate analysis. Statistical analyses using standard tests (χ^2, t test) were performed where appropriate. Significance was defined as $P < 0.05$. Statistical analyses were performed using StatView 5.0 Windows (SAS Institute Inc., Cary, NY, United States).

RESULTS

Analysis of AFP mRNA levels in bone marrow

The mean AFP mRNA/GAPDH ratio in the bone marrow (BM-AFP mRNA) of HCC patients, as determined by real-time quantitative RT-PCR, was 3469.27×10^{-7} (range: 0-348 526.19×10^{-7}). The cut-off value of the BM-AFP mRNA level was set at 1.92×10^{-7} (with reference to a previous report)[13]. The HCC patients were then divided into two groups according to this cut-off value. Accordingly, 80 patients (70.2%) were found to be negative for BM-AFP mRNA and 34 patients (29.8%), assigned to the "High" group, were positive for this transcript.

Expression of AFP mRNA in peripheral blood

No AFP mRNA was detectable in the peripheral blood of the control patients, therefore, the cut-off value for AFP mRNA/GAPDH in the peripheral blood (PH-AFP mRNA) was set at zero. Accordingly, six patients (5.4%) were found to be positive and 105 (94.6%) were negative for AFP mRNA. Due to some sampling loss, peripheral blood samples were unavailable for three patients.

Expression of VEGFR-1 mRNA in bone marrow

The mean VEGFR-1 mRNA/GAPDH in the bone marrow (BM-VEGFR-1 mRNA) of normal controls, again determined by real-time quantitative RT-PCR measurements, was 0.1497×10^{-3} (range: 0.0212×10^{-3} to 0.3213×10^{-3}). The mean BM-VEGFR-1 mRNA level in the HCC patients was 3.8474×10^{-3} (range: 0.3481×10^{-3} to

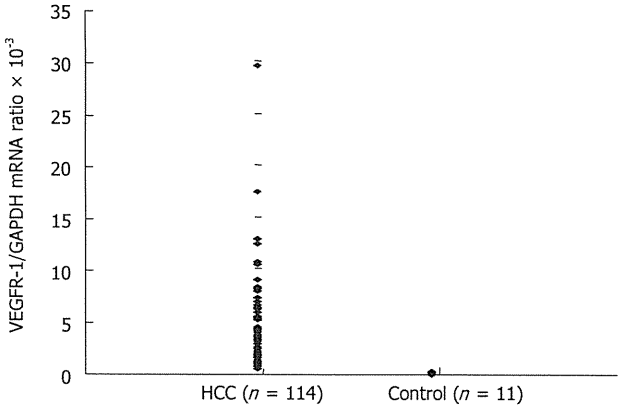

Figure 1 Expression of vascular endothelial growth factor receptor-1 mRNA in bone marrow detected by real-time quantitative reverse transcription polymerase chain reaction. The mean VEGFR-1/GAPDH mRNA ratio in the bone marrow (BM-VEGFR-1 mRNA) of normal controls was 0.1497 × 10^{-3} (range: 0.0212 × 10^{-3}-0.3213 × 10^{-3}). The mean BM-VEGFR-1 mRNA level in HCC patients was measured at 3.8474 × 10^{-3} (range: 0.3481 × 10^{-3}-29.5885 × 10^{-3}). HCC: Hepatocellular carcinoma; VEGFR: Vascular endothelial growth factor receptor; BM: Bone marrow; GAPDH: Glyceraldehyde-3-phosphate dehydrogenase.

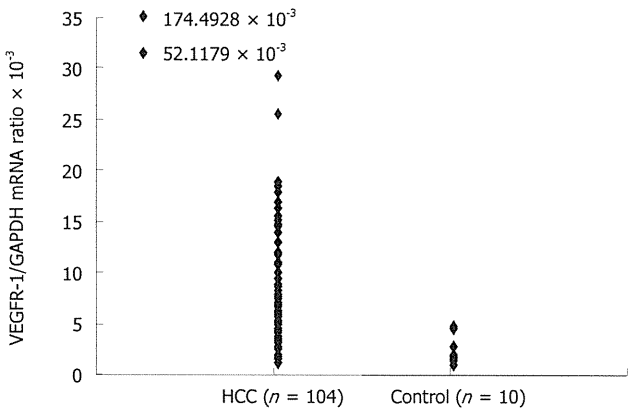

Figure 2 Expression of vascular endothelial growth factor receptor-1 mRNA in peripheral blood detected by real-time quantitative real-time quantitative reverse transcription polymerase chain reaction. The mean VEGFR-1/GAPDH mRNA ratio in the peripheral blood (PH-VEGFR-1 mRNA) of normal controls was 2.4944 × 10^{-3} (range: 1.0730 × 10^{-3}-4.6958 × 10^{-3}). The mean PH-VEGFR-1 mRNA level in HCC patients was 9.1285 × 10^{-3} (range: 1.2774 × 10^{-3}-174.4928 × 10^{-3}). HCC: Hepatocellular carcinoma; VEGFR: Vascular endothelial growth factor receptor; PH: Peripheral blood; GAPDH: Glyceraldehyde-3-phosphate dehydrogenase.

29.5885 × 10^{-3}). The mean BM-VEGFR-1 mRNA level of all HCC patients was higher than that of the normal controls (Figure 1). The HCC patients were then divided into two groups ("High" and "Low") according to their BM-VEGFR-1 mRNA level; the cut-off value was 1.5664 × 10^{-3}, which was the 25th percentile value of the BM-VEGFR-1 mRNA levels in the HCC cohort. The number of patients in the High group was 81 (71.1%) and 33 (28.9%) were assigned to the Low group.

Expression of VEGFR-1 mRNA in peripheral blood

The mean VEGFR-1 mRNA/GAPDH ratio in the peripheral blood (PH-VEGFR-1 mRNA) of the normal controls was 2.4944 × 10^{-3} (range: 1.0730 × 10^{-3} to 4.6958 × 10^{-3}). The mean PH-VEGFR-1 mRNA level in the HCC patients was 9.1285 × 10^{-3} (range: 1.2774 × 10^{-3} to 174.4928 × 10^{-3}). The PH-VEGFR-1 mRNA level of almost all HCC patients was higher than that of the normal controls (Figure 2). The HCC patients were divided into high and low groups according to their PH-VEGFR-1 mRNA level. The cut-off value was 4.0238 × 10^{-3}, which was in the 25th percentile of the PH-VEGFR-1 mRNA level of HCC patients. The number of patients in the high group was 78 (75.0%) with 26 (25.0%) placed in the Low group. Peripheral blood samples were available for 104 patients only.

Clinical significance of the BM- and PH-VEGFR-1, and BM- and PH-AFP mRNA levels

The status of the BM-AFP mRNA levels was correlated with microscopically detectable portal invasion, whereas that of PH-AFP mRNA was found to correlate with the serum AFP and AFP-L3 levels, the number of tumors, microscopic portal invasion, and microscopic intrahepatic metastasis (Table 1). The number of tumors, serum albumin level, and a noncancerous liver were significantly correlated with the BM-VEGFR-1 mRNA level (Table 2).

Patient outcomes

Mortality: By the end of our study, 42 of the HCC patients under analysis had died; 35 from HCC, three from liver failure and four from another malignant disease. The 1-, 2- and 3-year patient survival rates for this cohort were determined to be 92.1%, 85.9% and 78.7%, respectively.

HCC recurrence: HCC recurred in 80 patients (70.2%); in the remnant liver in 48 cases (60%), in the remnant liver and remote tissue in 20 (25%), and in the remote tissue alone in 12 (15%). The 1-, 2- and 3-year DFS rates were 67.5%, 49.8% and 34.4%, respectively. We found a significant tendency for patients who were positive for BM-AFP mRNA to experience recurrence within 1 year of their surgery compared with patients who were negative for this transcript (Table 3).

HCC classification according to VEGFR-1 and AFP mRNA status

Patients were classified into four groups according to the level/status of their BM-VEGFR-1 and BM-AFP mRNA as follows: group A (n = 23), BM-VEGFR-1/BM-AFP mRNA = low/negative; group B (n = 57) high/negative; group C (n = 10) low/positive; group D (n = 24), high/positive. This classification was correlated with disease recurrence within or more than 1 year after surgery. Significantly, in the groups in which patients were negative for BM-AFP mRNA, only three patients (13.0%) experienced recurrence in group A, whereas 17 (29.0%) in group B experienced recurrence within 1 year of surgery (Table 3). Classification of the HCC cases in the current study cohort by their PH-VEGFR-1 and BM-AFP (P = 0.1024), BM-VEGFR-1 and PH-AFP (P = 0.2100), and